frontiers in Neuroscience

ORIGINAL RESEARCH
published: 03 July 2019
doi: 10.3389/fnins.2019.00633

Meta-Analysis of Gene Expression and Identification of Biological Regulatory Mechanisms in Alzheimer's Disease

Lining Su[1], *Sufen Chen*[2], *Chenqing Zheng*[3], *Huiping Wei*[1]* *and Xiaoqing Song*[1]

[1] Department of Basic Medicine, Hebei North University, Zhangjiakou, China, [2] Institute of Educational Science, Zhangjiakou, China, [3] Shenzhen RealOmics (Biotech) Co., Ltd., Shenzhen, China

Alzheimer's disease (AD), also known as senile dementia, is a progressive neurodegenerative disease. The etiology and pathogenesis of AD have not yet been elucidated. We examined common differentially expressed genes (DEGs) from different AD tissue microarray datasets by meta-analysis and screened the AD-associated genes from the common DEGs using GCBI. Then we studied the gene expression network using the STRING database and identified the hub genes using Cytoscape. Furthermore, we analyzed the microRNAs (miRNAs), long non-coding RNAs (lncRNAs), and single nucleotide polymorphisms (SNPs) associated with the AD-associated genes, and then identified feed-forward loops. Finally, we performed SNP analysis of the AD-associated genes. Our results identified 207 common DEGs, of which 57 have previously been reported to be associated with AD. The common DEG expression network identified eight hub genes, all of which were previously known to be associated with AD. Further study of the regulatory miRNAs associated with the AD-associated genes and other genes specific to neurodegenerative diseases revealed 65 AD-associated miRNAs. Analysis of the miRNA associated transcription factor-miRNA-gene-gene associated TF (mTF-miRNA-gene-gTF) network around the AD-associated genes revealed 131 feed-forward loops (FFLs). Among them, one important FFL was found between the gene *SERPINA3*, hsa-miR-27a, and the transcription factor MYC. Furthermore, SNP analysis of the AD-associated genes identified 173 SNPs, and also found a role in AD for miRNAs specific to other neurodegenerative diseases, including hsa-miR-34c, hsa-miR-212, hsa-miR-34a, and hsa-miR-7. The regulatory network constructed in this study describes the mechanism of cell regulation in AD, in which miRNAs and lncRNAs can be considered AD regulatory factors.

Keywords: Alzheimer's disease, long non-coding RNA, microRNA, single nucleotide polymorphisms, network, meta-analysis

OPEN ACCESS

Edited by:
Cristian Bonvicini, Centro San Giovanni di Dio Fatebenefratelli (IRCCS), Italy

Reviewed by:
Nadia Cattane, Centro San Giovanni di Dio Fatebenefratelli (IRCCS), Italy
Fang Ding, Shenzhen University, China

***Correspondence:**
Huiping Wei
1931451387@qq.com

Specialty section:
This article was submitted to Neurogenomics, a section of the journal Frontiers in Neuroscience

Received: *15 February 2019*
Accepted: *31 May 2019*
Published: *03 July 2019*

Citation:
Su L, Chen S, Zheng C, Wei H and Song X (2019) Meta-Analysis of Gene Expression and Identification of Biological Regulatory Mechanisms in Alzheimer's Disease. Front. Neurosci. 13:633. doi: 10.3389/fnins.2019.00633

INTRODUCTION

Alzheimer's disease (AD) is the most well-reported neurodegenerative disease, and seriously affects patients' ability to perform daily activities. The characteristic pathological changes of AD are the formation of extracellular amyloid plaques by abnormal amyloid beta accumulation, the formation of intracellular neurofibrillary tangles by tau hyperphosphorylation, and neuronal loss

with gliosis proliferation (Huttenrauch et al., 2018). The etiology and pathogenesis of AD have not yet been elucidated.

To identify the genetic variation in AD, large cohort studies have been carried out. The expression of stromal interaction molecule 1 (STIM1) protein decreases with the progression of neurodegeneration in AD by triggering voltage-regulated Ca^{2+} entry-dependent cell death (Pascual-Caro et al., 2018). The cerebrospinal fluid levels of C-X3-C motif chemokine ligand 1 which is a chemokine expressed by neurons, are decreased in AD dementia patients compared with controls (Perea et al., 2018). Genome-wide association studies (GWAS) studies have also revealed that some single nucleotide polymorphisms (SNPs) contribute to AD disease onset. These include common variants such as estrogen receptor 1 (*ESR1*), presenilin 1 (*PSEN1*), cholinergic receptor muscarinic 2 (*CHRM2*), cholinergic receptor muscarinic 3 (*CHRM3*), apolipoprotein E (*APOE*), apolipoprotein C1 (*APOC1*), and choline acetyltransferase (*CHAT*) (Zhou et al., 2014; Liu et al., 2016; Bagyinszky et al., 2018; Chee and Cumming, 2018; Li et al., 2018), and also rare variants in genes such as eukaryotic translation initiation factor 2 alpha kinase 3 (*EIF2AK3*) (Wong et al., 2018). EIF2AK3 is a single-pass type 1 membrane protein, which represses global protein synthesis as an endoplasmic reticulum stress sensor (Liu et al., 2012). Several SNPs within *EIF2AK3* appear to significantly increase the risk of AD (Liu et al., 2013), especially rs147458427, an SNP that changes arginine to histidine at amino acid 240 (R240H) (Wong et al., 2018). Although *EIF2AK3* polymorphisms are related to a risk of delayed AD (Liu et al., 2013), their function in neurodegenerative diseases is not very clear.

Different microRNAs (miRNAs) are also associated with the pathophysiology of several neurodegenerative diseases (Gaughwin et al., 2011; Zovoilis et al., 2011), including AD (Kumar and Reddy, 2018). miRNA-377 promotes cell proliferation and inhibits cell apoptosis by regulating the expression level of cadherin 13 (*CDH13*), thus participating in the development of AD (Liu et al., 2018). The level of miR-221 is downregulated in AD cases compared with controls, and it is potentially a new therapeutic target for increasing ADAM metallopeptidase domain 10 (ADAM10) levels in AD (Manzine et al., 2018).

Long non-coding RNAs (lncRNAs) are widely reported to be associated with various physiological and pathological processes, such as neurodegenerative diseases (Wang et al., 2016; Wang D. Q. et al., 2018). Brain cytoplasmic (BC) RNA is a lncRNA present at higher levels in the AD-affected region of the brain than in normal brain (Mus et al., 2007), and overexpression of BC in AD may cause synaptic/dendritic degeneratio (Wang H. et al., 2018).

miRNAs function by targeting mRNAs for cleavage or translational repression. lncRNAs may affect miRNA activity by chelating them, thereby upregulating the expression of the miRNA target genes. The study of gene regulatory networks is important for disease analysis (Rankin and Zorn, 2014). However, research on the association of these AD markers in the context of biological networks is limited. To understand AD correctly, regulatory networks involving genes, miRNAs, transcription factors (TF), and lncRNAs need to be studied.

Abbreviations: DEGs, differentially expressed genes; gTF, transcription factor associated with gene; lncRNA, long non-coding RNA; miRNA, microRNA; mTF, transcription factor associated with miRNA; AD, Alzheimer's disease; SNP, single nucleotide polymorphism; TF, transcription factor; PPI, protein–protein interaction; FFL, feed-forward loop.

MATERIALS AND METHODS

Microarray Data Collection

We used "Alzheimer" as a keyword to search for gene expression studies from different brain tissues in the NCBI-GEO database (http://www.ncbi.nlm.nih.gov/geo/). Only original experimental studies that screened for genes differing between AD and healthy humans were selected. Our criteria were as follows: (1) the type of dataset was expression profiling by array; (2) the brain regions were the entorhinal cortex (EC), hippocampus (HIP), and medial temporal gyrus (MTG); (3) for each brain tissue dataset, the total number of available samples were $\geq$10. Finally, the samples from seven studies including three tissues (EC, HIP, and MTG) were screened out. We then performed a meta-analysis of three datasets from EC tissue (GSE48350, GSE5281, and GSE26927), five datasets from HIP tissue (GSE5281, GSE36980, GSE1297, GSE29378, and GSE48350), and two datasets from MTG tissue (GSE5281 and GSE84422). A detailed description of the microarray datasets is presented in **Table 1**. Detailed descriptions of the samples, including the brain regions, sex, and mean age, are provided in **Table S1**.

Searches were executed up to October 2017.

Analysis of Individual Data

Background correction and normalization of each individual dataset were performed using Robust Multichip Averaging (RMA) (Taminau et al., 2012). The differentially expressed genes (DEGs) between AD and healthy control samples (HC) were computed using the limma package (Derkow et al., 2018) in R. Gene symbol probes without gene annotation were removed. When multiple probes were matched with the same gene, the average value was used as the expression value.

Meta-Analysis of DEGs

Datasets from the same brain region (EC, HIP, or MTG) were combined to perform the meta-analysis. Initially, the data files were normalized using RMA. The normalized datasets were then merged using Fisher's exact test in the MetaDE package (Wang et al., 2012). The differentially expressed genes (DEGs) between AD and HC were selected using a $P < 0.05$ as the cut-off (**Figure 1**). In addition, the heterogeneity tests and differential expression analysis for each gene were analyzed using the ES algorithm of the MetaDE package in R (Wang et al., 2012). When multiple probes were matched with the same gene, we chose the average fold change of each probe. The thresholds of homogeneity were set as meta fold change

TABLE 1 | Datasets used in the meta-analysis.

Brain Regions	GEO accession	Sample size (AD/control)	Platform	PMID
Entorhinal Cortex (EC)	GSE48350	AD = 15; HC = 39	GPL570: Affymetrix Human Genome U133 Plus 2.0 Array	23273601 (Berchtold et al., 2013)
	GSE5281	AD = 10; HC = 13	GPL570: Affymetrix Human Genome U133 Plus 2.0 Array	29937276 (Readhead et al., 2018)
	GSE26927	AD = 11; HC = 7	GPL6255: Illumina humanRef-8 v2.0 expression beadchip	25119539 (Durrenberger et al., 2015)
Hippocampus (HIP)	GSE5281	AD = 10; HC = 13	GPL570: Affymetrix Human Genome U133 Plus 2.0 Array	29937276 (Readhead et al., 2018)
	GSE36980	AD = 7; HC = 10	GPL6244: Affymetrix Human Gene 1.0 ST Array	23595620 (Hokama et al., 2014)
	GSE29378	AD = 31; HC = 32	GPL6947: Illumina HumanHT-12 V3.0 expression beadchip	23705665 (Miller et al., 2013)
	GSE48350	AD = 19; HC = 43	GPL570: Affymetrix Human Genome U133 Plus 2.0 Array	23273601 (Berchtold et al., 2013)
	GSE1297	AD = 22; HC = 9	GPL96: Affymetrix Human Genome U133A Array	14769913 (Blalock et al., 2004)
Medial temporal gyrus (MTG)	GSE5281	AD = 16; HC = 12	GPL570: Affymetrix Human Genome U133 Plus 2.0 Array	29937276 (Readhead et al., 2018)
	GSE84422	AD = 20; HC = 14	GPL96: Affymetrix Human Genome U133A Array	27799057 (Wang et al., 2016)

AD, Alzheimer's disease; HC, healthy control.

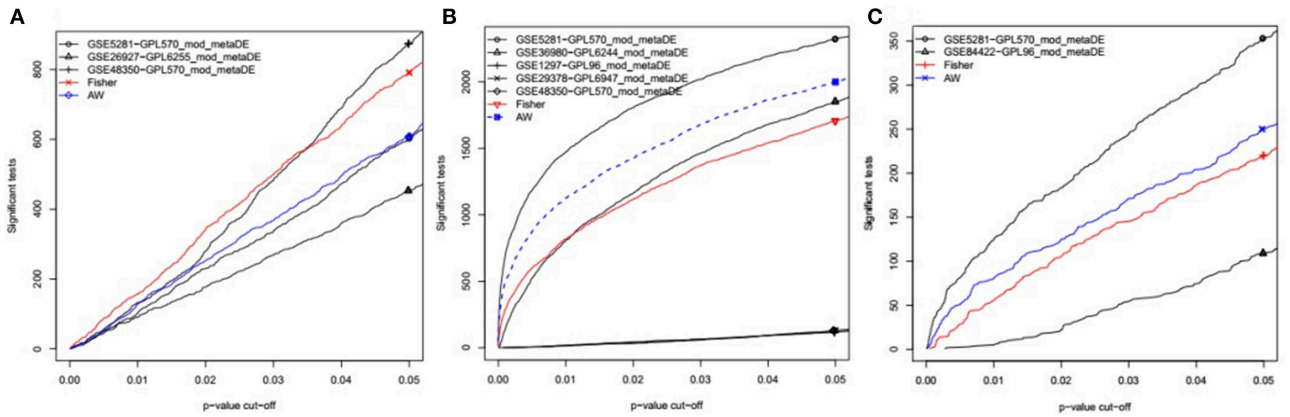

FIGURE 1 | *P*-value vs. number of detected DEGs for individual analysis as well as meta-analysis. In each individual dataset, moderated-t statistics was used to generate p-values while adaptive weight and Fisher's methods were utilized to combine these *p*-values for meta-analysis. This figure is generated using the "MetaDE" package in R. **(A)** The datasets from Entorhinal Cortex; **(B)** the datasets from Hippocampus; **(C)** the datasets from Medial temporal gyrus.

> 1, $tau^2 = 0$, and FDR > 0.05. The genes with $tau^2 = 0$ and FDR > 0.05 were considered homogeneous and unbiased, from which the genes with a $P < 0.05$ in the Fisher's exact test of the MetaDE package were selected as DEGs. Tau^2 represents the difference among study samples and reflects the heterogeneity between studies. The smaller the tau^2 value, the smaller the heterogeneity.

In this study, sub-meta-analyses on males and females with GSEs from different tissues were performed. The methods of normalization, meta-analysis, heterogeneity detection of each gene and threshold for selecting DEGs were the same as above.

RNA-Seq Data Analysis

We searched for gene expression studies from the NCBI-GEO database according to our criteria. The criteria were: (1) original studies between AD and healthy humans; (2) the type of dataset was expression profiling by high-throughput sequencing; (3) the brain regions used were EC, HIP, and MTG; (4) RNA-Seq data with poor quality controls were excluded. Finally, one gene expression dataset was selected, GSE67333, which uses samples from hippocampi brain regions and is based on GPL11154 platform information. Detailed information on these RNA-Seq samples is shown in **Table S2**. The available analyzed expression profiles of GSE67333 were used (Moradifard et al., 2018).

Construction of the DEG PPI Network, and Identification and Further Analysis of the Hub Nodes

STRING is a protein interaction network analysis tool. The latest version of the STRING database is 11.0 (Szklarczyk et al., 2019), which covers more than 5,090 species and 24.6 million proteins and supports the upload of genome-level data sets. To determine which proteins encoded by the DEGs play a leading role in AD, the DEGs were subjected to STRING v.11.0 with medium confidence scores of 0.4. To identify the hub nodes, we visualized the protein–protein interaction (PPI) network using Cytoscape v.3.6.0 software and analyzed the topological properties of these nodes using the Network Analyzer tool based on the degree parameter

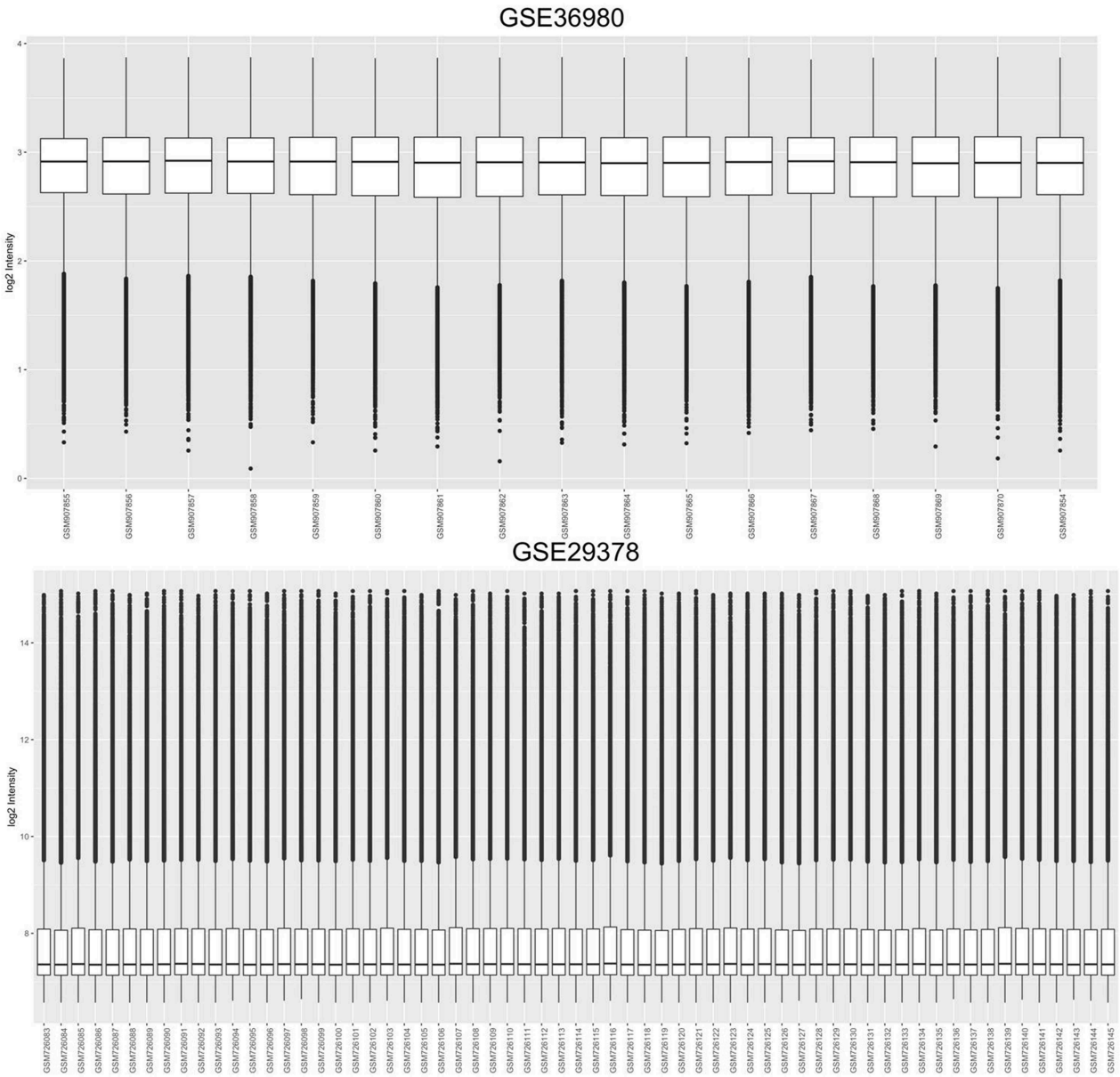

FIGURE 2 | Cassette figures of the expression data after standardization.

(Shannon et al., 2003). Then we selected the nodes with high degrees and high closeness centrality values as hubs. The degree is the number of protein-specific interactions, and a high value reflects an important role in the network. The closeness centrality reflects the ability of nodes to influence other nodes in the network, which reveals the centrality of the node in the network.

TABLE 2 | DEGs of Alzheimer's disease in different brain regions.

Brain partition	Up	Down
Entorhinal Cortex (EC)	120	63
Hippocampus (HIP)	4	5
Medial temporal gyrus (MTG)	14	1

Identification of DEGs Associated With AD and Other Neurodegenerative Diseases

The Gene Radar online tool in GCBI (Shanghai, China, https://www.gcbi.com.cn/gclib/html/index) mainly uses the disease classification in the Mesh database to mine correspondence between genes and diseases from the PubMed database. We used Gene Radar to identify the DEGs associated with AD and those associated with other neurodegenerative diseases.

TABLE 3 | Diferentially expressed genes (DEGs) identifed in the meta-analysis of AD datasets.

Brain tissue	Gene symbols	Meta. fold change	Meta. FDR	Meta. z-score	Brain tissue	Gene symbols	Meta. fold change	Meta. FDR	Meta. z-score
		Down regulated					**UP regulated**		
Entorhinal Cortex (EC)	*ABHD8*	−0.695534942	0.637337464	0.000948744	Entorhinal Cortex (EC)	*ENPP2*	0.44049447	0.429551194	0.033759913
	ACTR1A	−0.527310094	0.918943259	0.01124593		*FAM133B*	0.712276458	0.920723021	0.000694549
	ADAP1	−0.826978871	0.876417161	8.7236E-05		*FAM189A2*	0.489157939	0.410574925	0.018954003
	ALDOA	−0.384145613	0.425112103	0.062660907		*FANCL*	0.470511307	0.953386722	0.023061608
	ATP13A2	−0.762035644	0.766539678	0.000296769		*FBXO15*	0.993507129	0.757129441	3.75657E-06
	ATP5D	−0.723661334	0.534708953	0.000580599		*FUT9*	0.780769619	0.873935779	0.000212873
	BRSK2	−0.533706412	0.999573802	0.010248351		*GFAP*	0.398018735	0.376701655	0.054426496
	BSG	−0.516925038	0.413512963	0.013242341		*GTF2H5*	0.657325258	0.789398314	0.001738459
	C1QTNF4	−0.457508928	0.431360385	0.027673846		*HERC5*	0.574139491	0.947265969	0.005903665
	C9ORF16	−0.604569827	0.566387182	0.00393522		*HLA-A*	0.373842817	0.58003196	0.069323817
	CA11	−0.583952921	0.379126602	0.005356457		*HLA-DMA*	0.513914113	0.587127773	0.013644294
	CCDC3	−0.53490691	0.450261271	0.010464563		*HLA-DPA1*	0.353794692	0.657898571	0.084630186
	CHGA	−0.511634157	0.706121833	0.013873028		*HSPB8*	0.464862559	0.725668737	0.024925703
	COX7B	−0.633058899	0.522542766	0.002608732		*ID3*	0.556454024	0.75946288	0.007598297
	CPLX1	−0.491697637	0.654796636	0.017956424		*IFI16*	0.515223575	0.589948306	0.013365473
	DMTN	−0.517050939	0.54557447	0.013023207		*IFT80*	0.621059722	0.863851754	0.00303072
	DNM1	−0.748921362	0.851616972	0.000365222		*IGSF6*	0.565723712	0.935253446	0.006629518
	EDF1	−0.590415465	0.79983381	0.004719509		*IQCK*	0.824410953	0.785004124	9.22448E−05
	EIF5A	−0.561832967	0.763720591	0.007062777		*IRF8*	0.666513932	0.459048511	0.001602805
	EPHB6	−0.473978863	0.925286791	0.022141665		*KAT2B*	0.43895503	0.572883821	0.034051256
	FAIM2	−0.39169712	0.423434914	0.057746056		*KCTD12*	0.448754813	0.422874061	0.030866516
	FXYD7	−0.603890632	0.92041114	0.003888889		*KMT5B*	0.722220565	0.565274027	0.000604808
	GABRA1	−0.446962428	0.938560944	0.030608148		*LAP3*	0.600061529	0.752107238	0.004131397
	GAPDH	−0.543132906	0.903040583	0.009132231		*LBR*	0.545302628	0.633986877	0.009041239
	GNA11	−0.577416641	0.843517364	0.005654896		*LIX1*	0.5214595	0.717112961	0.012268136
	GNAS	−0.603746148	0.849586058	0.003904333		*LPAR4*	0.921307459	0.681435858	1.21045E-05
	GNB5	−0.411630184	0.446016846	0.046627431		*MAFB*	0.645061604	0.567530214	0.002210118
	GNG3	−0.511352374	0.60511663	0.013986977		*MAN2A1*	0.430556072	0.512746474	0.037462643
	HCFC1R1	−0.779144243	0.959187083	0.000221638		*MEGF10*	0.469347495	0.468585217	0.023860088
	HSPBP1	−0.526128712	0.837799088	0.011457968		*MYBPC1*	0.502311812	0.579998504	0.015894899
	INA	−0.386288506	0.407714233	0.061235913		*N4BP2L2*	0.898485485	0.893181433	1.66959E-05
	IPCEF1	−0.427095032	0.568091293	0.039036647		*NFASC*	0.519910402	0.47159205	0.012649219
	KCNH3	−0.689163117	0.88872707	0.001033475		*NPL*	0.585010189	0.930952647	0.005073462
	KCNS1	−0.420524054	0.753519306	0.041720093		*NQO1*	0.583983538	0.877051724	0.005170715
	L1CAM	−0.537297073	0.853172878	0.00989732		*NUP133*	0.628705637	0.535452706	0.002834544
	MAP1A	−0.665635022	0.662053461	0.001574005		*OGFRL1*	0.73737742	0.988179105	0.000443276
	MIF	−0.726002013	0.612623491	0.000561817		*P2RY1*	0.615041285	0.619500158	0.003352534
	MINK1	−0.41901789	0.512203346	0.042751064		*PALLD*	0.552681973	0.729315709	0.008066199
	MLF2	−0.631968567	0.729765354	0.002633776		*PCMTD2*	0.722905062	0.996225613	0.000571834
	MLST8	−0.808675599	0.408001512	0.000135237		*PIGF*	0.714748936	0.831142721	0.00067827
	NARS	−0.536469861	0.622164429	0.010066784		*PLEK*	0.631049594	0.92097513	0.002621254
	NDUFV3	−0.750515002	0.962465905	0.000351448		*PLSCR4*	0.499091341	0.456919204	0.01664371
	NPDC1	−0.560193708	0.812610721	0.007166708		*PLXDC2*	0.563414288	0.610862181	0.006953418
	NPM2	−0.692171755	0.892705473	0.000990483		*PPM1K*	0.663355287	0.794773659	0.001602805
	NRGN	−0.543671699	0.759036634	0.009171049		*PRDX1*	0.486533018	0.875508707	0.018985308
	NRSN2	−0.689295698	0.797483245	0.001049336		*PRDX6*	0.528459065	0.898873556	0.011077302
	NRXN2	−0.658068088	0.648530052	0.001734285		*PRPF38B*	0.717412208	0.47672117	0.000668253
	OTUB1	−0.510602162	0.838921288	0.013990734		*PTPN13*	0.740120096	0.847406651	0.000426997

(Continued)

TABLE 3 | Continued

Brain tissue	Gene symbols	Meta. fold change	Meta. FDR	Meta. z-score	Brain tissue	Gene symbols	Meta. fold change	Meta. FDR	Meta. z-score
		Down regulated					**UP regulated**		
	PCSK1N	−0.577285436	0.708629247	0.005726271		*PTTG1IP*	0.528946561	0.592564809	0.01120586
	POLR2I	−0.447268575	0.723136773	0.030829368		*QKI*	0.482455410	0.56935108	0.020327239
	PPFIA3	−0.588045143	0.568361574	0.004924869		*RAB10*	0.571514428	0.96471241	0.006130729
	RAD23A	−0.706497339	0.503752324	0.000808498		*RB1*	0.771349913	0.70327628	0.000265047
	RPH3A	−0.603970489	0.831838989	0.003941481		*RBL2*	0.596654578	0.955853017	0.004295016
	SEZ6L2	−0.760423859	0.845850174	0.000308039		*RHOBTB3*	0.517224591	0.635022215	0.012995242
	SLC17A6	−0.533301618	0.430952335	0.010548042		*RNF19A*	0.592985615	0.811236679	0.004594707
	SLC25A6	−0.655147169	0.610182759	0.001839469		*SERPINA3*	0.260148507	0.410252167	0.199003256
	SYN1	−0.500531256	0.401736659	0.01638868		*SFRP2*	0.710029305	0.949693908	0.000717923
	TMSB10	−0.532612324	0.697663977	0.010507137		*SLC16A9*	0.382811918	0.378195934	0.06339803
	TNPO2	−0.614679785	0.930625382	0.003314968		*SLC44A1*	0.638101475	0.762520335	0.002367894
	TOMM40	−0.738938287	0.985360607	0.000431171		*SLC47A2*	0.453485364	0.582897757	0.028596711
	TUBB4A	−0.489135484	0.590668267	0.018714834		*SMAD5*	0.727328341	0.605345958	0.000553469
	TUBB4B	−0.555933702	0.581279394	0.007710577		*SMC3*	0.704413915	0.748404935	0.000804324
	USP11	−0.458379228	0.748899819	0.026995158		*SMG1*	0.753030042	0.746878908	0.000341013
Hippocampus (HIP)	*RPS27A*	−0.506389968	0.498368501	0.000441679		*SOX9*	0.426447386	0.834971993	0.038857167
	TPD52L2	−0.495625518	0.513661726	0.000568354		*SPARC*	0.434472551	0.909292556	0.035391101
	IFI27	−0.457966173	0.686297499	0.001275153		*SPATA13*	0.71020661	0.728056464	0.000732949
	HBB	−0.386701035	0.420669794	0.005961549		*SPP1*	0.493881628	0.452317782	0.017825778
	NCAN	−0.237122792	0.418570953	0.082322179		*SRSF6*	0.458207354	0.831801769	0.026846982
Medial temporal gyrus(MTG)	*BAIAP3*	−0.653066361	0.435361527	0.006816604		*STARD7*	0.494066945	0.774264489	0.017368311
						STOM	0.454651040	0.432990835	0.028810836
		Up regulated				*SUMF1*	0.745609227	0.904439144	0.000385675
Entorhinal Cortex (EC)	*ACADM*	0.509396446	0.472281771	0.014636865		*TAC1*	0.391075996	0.474031506	0.057949745
	ACTL6A	0.63989583	0.918366926	0.002292345		*TJP2*	0.532971400	0.750652089	0.010483346
	ADAMTSL3	0.55218035	0.526447536	0.008121713		*TMEM123*	0.62618571	0.657410829	0.002886301
	ADAP2	0.58201966	0.741648989	0.00536564		*TPD52L1*	0.489260339	0.506535512	0.018809583
	AK3	0.624295669	0.436260102	0.003014442		*TPT1*	0.300133425	0.368223777	0.141755572
	AKR1C3	0.610232089	0.96965544	0.003533684		*TRIM22*	0.678534839	0.832321099	0.001261374
	ALDH9A1	0.632866364	0.75439915	0.002612489		*TRMT13*	0.793756883	0.369197713	0.000174472
	AMOTL2	0.525992143	0.439842541	0.011663327		*TSPAN6*	0.629323862	0.934431325	0.002691794
	ANGPT1	0.541370626	0.948471299	0.009286251		*UNC50*	0.538042189	0.675647763	0.009896486
	ANXA5	0.519090679	0.491664199	0.012875449		*VPS13C*	0.575598517	0.383372507	0.006035562
	APBB1IP	0.608077987	0.953355887	0.003667668		*WDR11*	0.838741219	0.890945758	6.72009E-05
	APLNR	0.370607123	0.853230372	0.070987979		*WRN*	0.697603632	0.573479036	0.0009141
	ARFGAP3	0.701645153	0.629505964	0.000882795		*ZFAND6*	0.669587769	0.788327401	0.001442107
	ARRDC4	0.537624139	0.502111086	0.00999833		*ZNF536*	0.408408649	0.397147119	0.048474831
	ATG4C	0.624765761	0.440666196	0.002969363		*ZNF770*	0.875598858	0.482428475	3.13048E-05
	ATRAID	0.601603100	0.775419452	0.004065448	Hippocampus (HIP)	*PCSK1N*	0.225974152	0.416500814	0.09711283
	B2M	0.353023046	0.579830231	0.085440354		*GJA1*	0.252228568	0.674305099	0.035832633
	BBOX1	0.644908898	0.465640403	0.002237249		*MT1M*	0.289185091	0.603279837	0.035832633
	BMI1	0.542056551	0.673043701	0.00935053		*PLSCR4*	0.29691696	0.406351363	0.031675355
	C3	0.421657492	0.839037764	0.040981301	Medial temporal gyrus(MTG)	*AEBP1*	0.70464363	0.521628759	0.003562337

(Continued)

TABLE 3 | Continued

Brain tissue	Gene symbols	Meta. fold change	Meta. FDR	Meta. z-score	Brain tissue	Gene symbols	Meta. fold change	Meta. FDR	Meta. z-score
		Down regulated					UP regulated		
	C5ORF15	0.804720546	0.741920597	0.000134819		*AFFX-HUMRGE/M10098_3_AT*	0.368444288	0.511222692	0.120022659
	CAPN2	0.535982721	0.760836799	0.010108106		*AFFX-HUMRGE/M10098_5_AT*	0.550884703	0.476493887	0.021509016
	CAPS	0.483265112	0.560111705	0.019921529		*AFFX-HUMRGE/M10098_M_AT*	0.467365996	0.623774962	0.050219844
	CD81	0.51520138	0.871213337	0.013160531		*COX17*	0.818729013	0.427171437	0.000795487
	CEBPB	0.380312809	0.378471552	0.065611904		*EEF2*	0.386796708	0.358680034	0.103799055
	CLCA4	0.65055172	0.434917261	0.002025628		*GOT2*	0.468316719	0.34099237	0.050357246
	CLU	0.447778971	0.448785848	0.030793889		*HBA1*	0.715632134	0.485832639	0.003132774
	CMTR2	0.629566266	0.552935904	0.00274856		*HSPB1*	0.470339479	0.624218434	0.048780735
	COMMD3	0.534472888	0.71040471	0.010343935		*MT3*	0.469118942	0.458310927	0.049672645
	CP	0.523351329	0.715531248	0.011868269		*NME2*	0.647538352	0.353484653	0.007327162
	CSRP2	0.533389066	0.653399315	0.010396527		*SEPP1*	0.517802828	0.438589877	0.03046524
	DDIT4L	0.461914904	0.984152235	0.025550129		*SEPW1*	0.477043287	0.45908091	0.045928551
	DOCK4	0.684322338	0.516002378	0.001146172		*ZBTB16*	0.515674996	0.345619847	0.031356668
	DYNLT1	0.614852884	0.938093709	0.003331664					

The DEGs were listed based on homogeneity detection FDR and meta-analysis fold change. AD, Alzheimer's disease; HC, healthy control.

Analysis of miRNAs Associated With the AD-Associated and Other Neurodegenerative Disease-Associated DEGs, and of lncRNAs Associated With These miRNAs

DIANA-Tarbase v.8.0, containing 670,000 unique experimentally-supported miRNA–gene pairs (Karagkouni et al., 2018), was used to analyze the miRNAs associated with the AD-associated and other neurodegenerative disease-associated DEGs. Then, the miRNAs associated with AD and other neurodegenerative diseases were filtered using the miRdSNP v.11.03 online database (Bruno et al., 2012).

DIANA-LncBase Experimental v.2, which provides more than 70,000 low- and high-throughput experimentally-supported miRNA–lncRNA interactions (Paraskevopoulou et al., 2016), was used to examine interactions between lncRNAs and these miRNAs. In our study, experimentally validated (prediction score $\geq$ 0.90) lncRNAs in human brain tissue were selected.

Differentially Expressed miRNAs in AD by High-Throughput Data

High-throughput data on miRNAs in AD is rare, so we collected only one miRNA microarray dataset in GEO (GSE16759), which studied miRNA expression in AD patients and controls (Nunez-Iglesias et al., 2010). The differentially expressed miRNAs were screened using the GEO2R tool, which is an interactive web tool based on GEO query and limma R packages (Davis and Meltzer, 2007).

Analysis of Transcription Factors Associated With the AD-Associated/Other Neurodegenerative Disease-Associated DEGs and AD-Associated/Other Neurodegenerative Disease-Associated miRNAs

To study the molecular regulatory mechanisms in AD, we built regulatory networks comprising AD-associated/other neurodegenerative disease-associated DEGs, TFs associated with these genes (gTFs), AD-associated/other neurodegenerative disease-associated miRNAs targeting these genes, and TFs related to these miRNAs (mTFs).

Information on the TF binding sites associated with these genes were studied using TRANSFAC (Fogel et al., 2005) based on the Match™ algorithm. The TRANSFAC database comprises eukaryotic transcription factors, DNA binding sites, and their effects on gene expression (Fogel et al., 2005). In our study, the matrix similarity score (MSS) and the core similarity score (CSS) were used to estimate the result. The threshold values of MSS and CSS for selection were both score = 1.

Regulatory information on the TFs associated with these miRNAs was analyzed using TransmiR v.2.0 database, an updated TF–miRNA regulation database (Wang et al., 2010). In our study, the literature-curated TF–miRNA regulations and the TF–miRNA interactions from ChIP-Seq evidence in human neural tissue were selected.

Verification of FFL Between the Gene SERPINA3, hsa-miR-27a and TF MYC

In order to verify the positive finding, FFL between the gene SERPINA3, hsa-miR-27a, and TF MYC, we collected GSE16759

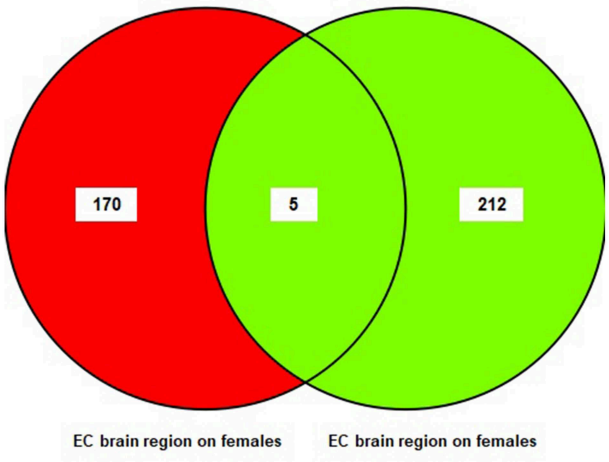

FIGURE 3 | The number of common genes obtained from entorhinal Cortex (EC) in females and males visualized by a Venn diagram.

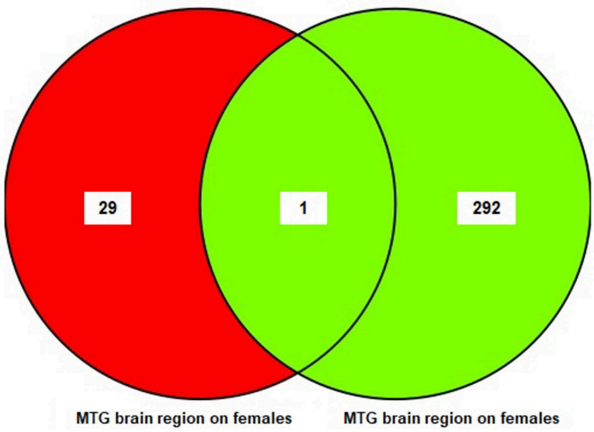

FIGURE 4 | The number of common genes obtained from medial temporal gyrus (MTG) in females and males visualized by a Venn diagram.

dataset, which jointly profiled mRNA and miRNA expression in AD patients and controls (Nunez-Iglesias et al., 2010). The differentially expressed mRNA and miRNAs were screened using the GEO2R tool (Davis and Meltzer, 2007).

To further verify the positive finding, GSE46579 dataset which studied miRNA expression in AD patients and controls blood and GSE97760 dataset which studied mRNA expression in AD patients and controls blood were collected. The available analyzed expression profiles of GSE46579 were used (Leidinger et al., 2013). The differentially expressed mRNA were also screened using the GEO2R tool.

SNP Analysis of the AD-Associated DEGs

To identify the AD-associated SNPs, SNP analysis of the AD-associated DEGs was performed. We used miRdSNP v.11.03 (Bruno et al., 2012) and LincSNP v.2.0 (Ning et al., 2014) to identify AD-associated SNPs associated with AD-associated DEGs (Yousef, 2015) Chromosome locus and allele gene information associated with each of the SNPs were received from dbSNP database (https://www.ncbi.nlm.nih.gov/snp/?term=).

RESULTS

Analysis of Individual Datasets

Each individual dataset selected for use in the meta-analysis were corrected and normalized using the oligopackage (Liu et al., 2018) in R. All results are shown in **Additional Figures**, parts of which are shown in **Figure 2**.

Meta-Analysis of DEGs

To identify common DEGs in different brain regions between AD and healthy controls, microarray datasets (**Table 1**) from three different brain regions (EC, HIP, and MTG) were meta-analyzed using the "MetaDE" package in R. With the threshold of $P < 0.05$ in Fisher's exact test, 781 DEGs in the EC brain region, 1707 DEGs in the HIP brain region and 220 DEGs in the MTG brain region were obtained. Then, with the homogeneity thresholds of meta fold change > 1, $\text{tau}^2 = 0$, and FDR > 0.05, the DEGs with $P < 0.05$ in the meta-analysis from each tissue were collected and are shown in **Table 2**. The final results identified 183 DEGs in the EC brain region (120 upregulated and 63 downregulated), nine DEGs in the HIP brain region (four upregulated and five downregulated) and 15 DEGs in the MTG brain region (14 upregulated and one downregulated). A total of 207 DEGs were identified between the AD and HC samples (**Table 2**). More details about the DEGs are presented in **Table 3**, including the meta-expression between AD and HC and the Qpval in the meta-analysis. These 207 genes were identified as DEGs for the subsequent analysis.

A sub-meta-analysis on females and males was performed using datasets from each brain region (EC, HIP, and MTG). The results of the sub-meta-analysis of the EC brain region in males and females revealed that there were 217 DEGs in males (176 upregulated and 41 downregulated), of which 212 were male-specific, and 175 DEGs in females (five upregulated and 170 downregulated), of which 170 were female-specific (**Table S3**). Only five common DEGs were identified in females and males. The result of this analysis is also shown in a Venn diagram (**Figure 3**).

The results of the sub-meta-analysis of the HIP brain region in males and females showed that there were 11 DEGs in males (one upregulated and 10 downregulated), and 28 DEGs in females (10 upregulated and 18 downregulated). No overlapping DEGs were obtained between females and males (**Table S4**).

The results of the sub-meta-analysis of the MTG brain region in males and females showed that there were 293 DEGs in males (11 upregulated and 282 downregulated), and 30 DEGs in females (19 upregulated and 11 downregulated) (**Table S5**). Only one common DEG was identified in females and males. The result of this analysis is also shown in a Venn diagram (**Figure 4**).

TABLE 4 | AD and other neurodegenerative diseases associate genes identified from DEGs using GCBI online software.

Expressionin meta-analysis	Gene symbol	Brain partition	Gene name	Corresponding neurodegenerative disease
Down-regulated	*ADAP1*	EC	ArfGAP with dual PH domains 1	AD
	MLST8	EC	MTOR associated protein, LST8 homolog	AD
	HCFC1R1	EC	Host cell factor C1 regulator 1	AD
	NDUFV3	EC	NADH:ubiquinone oxidoreductase subunit V3	AD
	DNM1	EC	Dynamin 1	AD
	TOMM40	EC	Translocase of outer mitochondrial membrane 40	AD
	RAD23A	EC	RAD23 homolog A, nucleotide excision repair protein	AD
	RPH3A	EC	Rabphilin 3A	AD
	FXYD7	EC	FXYD domain containing ion transport regulator 7	AD
	GNAS	EC	GNAS complex locus	AD
	PCSK1N	EC	Proprotein convertase subtilisin/kexin type 1 inhibitor	AD
	TUBB4B	EC	Tubulin beta 4B class IVb	AD
	NRGN	EC	Neurogranin	AD
	GAPDH	EC	Glyceraldehyde-3-phosphate dehydrogenase	AD
	L1CAM	EC	L1 cell adhesion molecule	AD
	BRSK2	EC	BR serine/threonine kinase 2	AD
	SLC17A6	EC	Solute carrier family 17 member 6	AD
	HSPBP1	EC	HSPA (Hsp70) binding protein 1	AD
	DMTN	EC	Dematin actin binding protein	AD
	SYN1	EC	Synapsin I	AD
	GNB5	EC	G protein subunit beta 5	AD
	INA	EC	Internexin neuronal intermediate filament protein alpha	AD
	RPS27A	HIP	Ribosomal protein S27a	AD
	ATP13A2	EC	ATPase 13A2	PD
	MAP1A	EC	Microtubule associated protein 1A	PD
	SLC25A6	EC	Solute carrier family 25 member 6	PD
	ATP5D	EC	ATP synthase, H+ transporting, mitochondrial F1 complex, delta subunit	Multiple sclerosis
	MLF2	EC	Myeloid leukemia factor 2	Multiple sclerosis
	CA11	EC	Carbonic anhydrase 11	Multiple sclerosis
	ACTR1A	EC	ARP1 actin-related protein 1 homolog A, centractin alpha	Multiple sclerosis
	OTUB1	EC	OTU deubiquitinase, ubiquitin aldehyde binding 1	Multiple sclerosis
	EPHB6	EC	EPH receptor B6	Multiple sclerosis
	C1QTNF4	EC	C1q and tumor necrosis factor related protein 4	Multiple sclerosis
	ALDOA	EC	Aldolase, fructose-bisphosphate A	Multiple sclerosis
	EDF1	EC	Endothelial differentiation related factor 1	Neurodegenerative disease
	NARS	EC	Asparaginyl-tRNA synthetase	Neurodegenerative disease
Up-regulated	*SERPINA3*	EC	Serpin family A member 3	AD
	SLC16A9	EC	Solute carrier family 16 member 9	AD
	TAC1	EC	Tachykinin precursor 1	AD
	GFAP	EC	Glial fibrillary acidic protein	AD
	MAN2A1	EC	Mannosidase alpha class 2A member 1	AD
	SRSF6	EC	Serine and arginine rich splicing factor 6	AD
	HSPB8	EC	Heat shock protein family B (small) member 8	AD
	MEGF10	EC	Multiple EGF like domains 10	AD
	PRDX1	EC	Peroxiredoxin 1	AD
	CP	EC	Ceruloplasmin	AD

(Continued)

TABLE 4 | Continued

Expressionin meta-analysis	Gene symbol	Brain partition	Gene name	Corresponding neurodegenerative disease
	PRDX6	EC	Peroxiredoxin 6	AD
	CAPN2	EC	Calpain 2	AD
	PLXDC2	EC	Plexin domain containing 2	AD
	IGSF6	EC	Immunoglobulin superfamily member 6	AD
	RAB10	EC	RAB10, member RAS oncogene family	AD
	ADAP2	EC	ArfGAP with dual PH domains 2	AD
	NPL	EC	N-acetylneuraminate pyruvate lyase	AD
	LAP3	EC	Leucine aminopeptidase 3	AD
	ATRAID	EC	All-trans retinoic acid induced differentiation factor	AD
	APBB1IP	EC	Amyloid beta precursor protein binding family B member 1 interacting protein	AD
	DYNLT1	EC	Dynein light chain Tctex-type 1	AD
	ARFGAP3	EC	ADP ribosylation factor GTPase activating protein 3	AD
	FAM133B	EC	Family with sequence similarity 133 member B	AD
	IQCK	EC	IQ motif containing K	AD
	WDR11	EC	WD repeat domain 11	AD
	CLU	EC	Clusterin	AD
	B2M	EC	Beta-2-microglobulin	AD
	MT3	MTG	Metallothionein 3	AD
	SEPP1	MTG	Selenoprotein P	AD
	NME2	MTG	NME/NM23 nucleoside diphosphate kinase 2	AD
	EEF2	MTG	Eukaryotic translation elongation factor 2	AD
	PCSK1N	HIP	Proprotein convertase subtilisin/kexin type 1 inhibitor	AD
	MT1M	HIP	Metallothionein 1M	AD
	GJA1	HIP	Gap junction protein alpha 1	AD
	STARD7	EC	StAR related lipid transfer domain containing 7	PD
	MYBPC1	EC	Myosin binding protein C, slow type	PD
	AMOTL2	EC	Angiomotin like 2	PD
	VPS13C	EC	Vacuolar protein sorting 13 homolog C	PD
	RNF19A	EC	Ring finger protein 19A, RBR E3 ubiquitin protein ligase	PD
	NUP133	EC	Nucleoporin 133	PD
	PCMTD2	EC	Protein-L-isoaspartate (D-aspartate) O-methyltransferase domain containing 2	PD
	HLA-A	EC	Major histocompatibility complex, class I, A	Multiple sclerosis
	ZNF536	EC	Zinc finger protein 536	Multiple sclerosis
	STOM	EC	Stomatin	Multiple sclerosis
	QKI	EC	QKI, KH domain containing RNA binding	Multiple sclerosis
	CAPS	EC	Calcyphosine	Multiple sclerosis
	SPP1	EC	Secreted phosphoprotein 1	Multiple sclerosis
	ACADM	EC	Acyl-CoA dehydrogenase, C-4 to C-12 straight chain	Multiple sclerosis
	HLA-DMA	EC	Major histocompatibility complex, class II, DM alpha	Multiple sclerosis
	NFASC	EC	Neurofascin	Multiple sclerosis
	PLEK	EC	Pleckstrin	Multiple sclerosis; HD
	ACTL6A	EC	Actin like 6A	Multiple sclerosis; PD
	GTF2H5	EC	General transcription factor IIH subunit 5	Multiple sclerosis
	IRF8	EC	Interferon regulatory factor 8	Multiple sclerosis
	TRIM22	EC	Tripartite motif containing 22	Multiple sclerosis
	PRPF38B	EC	Pre-mRNA processing factor 38B	Multiple sclerosis

(Continued)

TABLE 4 | Continued

Expressionin meta-analysis	Gene symbol	Brain partition	Gene name	Corresponding neurodegenerative disease
	KMT5B	EC	Lysine methyltransferase 5B	Multiple sclerosis
	AK3	EC	Adenylate kinase 3	HD
	PPM1K	EC	Protein phosphatase, Mg2+/Mn2+ dependent 1K	HD
	FUT9	EC	Fucosyltransferase 9	HD
	FAM189A2	EC	Family with sequence similarity 189 member A2	Neurodegenerative disease
	ATG4C	EC	Autophagy related 4C cysteine peptidase	Neurodegenerative disease
	TSPAN6	EC	Tetraspanin 6	Neurodegenerative disease
	SLC44A1	EC	Solute carrier family 44 member 1	Neurodegenerative disease
	SUMF1	EC	Sulfatase modifying factor 1	Neurodegenerative disease

Analysis of Gene Expression in AD by RNA Sequencing

To further validate the results from the microarray data with public RNA-Seq data, we selected datasets that used the same brain regions as the microarray datasets. Hence, the DEGs between AD and HC were analyzed in the GSE67333 RNA-Seq dataset. This revealed that 1102 DEGs were filtered from GSE67333 with a threshold of $P < 0.05$ and fold change ≥ 1.23 (Moradifard et al., 2018). Detailed information on these DEGs is shown in **Table S6**. Then, we analyzed the common DEGs between the RNA-Seq and microarray data, which revealed 72 common DEGs in the HIP brain region in both the RNA-Seq and microarray data.

Identification of AD-Associated or Other Neurodegenerative Disease-Associated DEGs

AD-associated and other neurodegenerative disease-associated genes were identified from the DEGs using the Gene Radar tool from the GCBI online software. Out of the 207 total DEGs, 57 had previously been shown to be associated with AD (AD-associated genes; 34 upregulated and 23 downregulated), and 43 DEGs had previously been shown to be associated with several other neurodegenerative diseases (other neurodegenerative disease-associated genes; 30 upregulated and 13 downregulated), such as multiple sclerosis, Parkinson's disease (PD) and Huntington disease (HD) (**Table 4**). Overall, the number of upregulated genes was greater than the number of downregulated genes. These AD-associated or other neurodegenerative disease-associated DEGs are important genes for further research. The detailed down/upregulated status of the 57 AD-associated DEGs in each individual dataset is provided in **Table 5**.

Analysis of the DEG PPI Network and Identification of Hub Nodes

The 207 DEGs were subjected to STRING v.11.0 to study the PPI network, and 154 nodes were sorted. The interaction network was then analyzed using the Network Analyzer tool (Shannon et al., 2003) (**Figure 5**). The 154 genes showed varying degrees of distribution, with a maximum degree of 39 and a minimum degree of 1. The upper eight nodes (top 5% of all nodes) with high degree and high closeness centrality values were chosen as hub nodes (**Table 6**). These eight hubs (*GAPDH*, *RPS27A*, *GFAP*, *B2M*, *CLU*, *EEF2*, *GJA1,* and *CP*) have all previously been found to be involved in the process of AD (Deane et al., 2005; Li et al., 2005; Olah et al., 2011; El Kadmiri et al., 2014; Guerreiro et al., 2015; Kamphuis et al., 2015; Almeida et al., 2018; Karagkouni et al., 2018).

The miRNAs Associated With the AD-Associated and Other Neurodegenerative Disease-Associated DEGs, and the lncRNAs Associated With These miRNAs

To investigate the interactions between the AD-associated DEGs and non-coding RNAs, miRNAs associated with these genes were analyzed using the DIANA-Tarbase v.8.0 database. Of these miRNAs, 48 miRNAs were related to AD (**Table 7**), and 22 miRNAs were associated with other neurodegenerative diseases, such as multiple sclerosis and Parkinson's disease (**Table 8**). To investigate the interactions between the other neurodegenerative disease-associated DEGs and non-coding RNAs, 17 miRNAs were identified as being related to AD (**Table 9**). Moreover, most of these miRNAs were in turn regulated by many lncRNAs.

Analysis of miRNA Expression in AD by High-Throughput Data

To study the predicted expression of the AD-associated miRNAs further, a GEO dataset (GSE16759) studying miRNA was analyzed. This revealed 870 differentially expressed miRNAs. Detailed information on these miRNAs is shown in **Table S7**. Then, we analyzed the miRNAs common to both GSE16759 and our AD-associated miRNAs, and detected 47 of our AD-associated miRNAs in the GEO data. The top 12 significant miRNAs common to both GSE16759 and our AD-associated miRNAs are listed in **Table 10**.

TABLE 5 | The down/up situation of 57 AD-associate genes identified in the meta-analysis in each individual dataset.

Down-regulated	Hippocampus (HIP)									
	GSE5281		GSE36980		GSE48350		GSE29378		GSE1297	
	log2FoldChange	*P*-Value	log2FoldChange	*P*-Value	log2FoldChange	*P*-Value	log2FoldChange	*P*-Value	log2FoldChange	*P*-Value
RPS27A	−0.726653445	0.037078998	0.006418053	0.634791602	0.162273062	0.00159256	4.70E-05	0.006604828	0.224013488	0.913570635
Up-regulated	**log2FoldChange**	***P*-Value**	**log2FoldChange**	***P*-Value**	**log2FoldChange**	***P*-Value**	**log2FoldChange**	***P*-Value**	**log2FoldChange**	***P*-Value**
PCSK1N	0.138069789	0.50703397	−0.031361177	0.057833175	−0.233532889	0.187009896	NA		−0.562365704	0.177607105
MT1M	0.705082952	0.092700761	0.047028345	0.282787829	0.125837365	0.739204026	0.134012269	0.872273811	−0.57594349	0.430641885
GJA1	0.321846385	0.423970204	0.04636156	0.176170552	−0.046712345	0.743685092	-0.017238343	0.444546304	0.03288786	0.614266746

Down-regulated	Entorhinal Cortex (EC)					
	GSE5281		GSE26927		GSE48350	
	log2FoldChange	*P*-Value	log2FoldChange	*P*-Value	log2FoldChange	*P*-Value
ADAP1	−0.975358771	0.000738556	−0.10598992	0.4322535	0.26177215	0.008467065
BRSK2	−2.877946644	2.47*E* − 05	−0.05492211	0.6649916	0.471708705	0.012467794
DMTN	−1.424808111	8.99*E* − 06	0.01319122	0.9421318	0.235990221	0.191857188
DNM1	−2.739879787	2.39*E* − 07	0.04539906	0.8220179	0.150042132	0.156014246
FXYD7	−1.927020252	0.00012567	0.12906713	0.4024216	0.421928539	0.067078593
GAPDH	−1.876446535	1.83*E* − 05	0.10665021	0.4125155	0.131208665	0.071996601
GNAS	−2.168431795	0.003326198	−0.55014104	0.3213458	0.101005549	0.082500384
GNB5	−2.629499459	0.000143728	0.05259637	0.6220857	0.267868945	0.177291265
HCFC1R1	−2.418575208	0.001577245	0.07272677	0.7672356	0.291574573	0.001166783
INA	−2.213790118	0.000286098	0.15823794	0.4368417	0.23025025	0.29758798
L1CAM	−2.253719243	3.32*E* − 08	0.09255605	0.6813247	0.215178049	0.254031866
MLST8	−1.080812867	0.000603178	−0.12108112	0.3325045	0.287724012	0.005909275
NDUFV3	−2.456436763	0.000139382	−0.04468396	0.8369119	0.290209615	0.000799514
NRGN	−1.93628633	0.004325631	−0.11981346	0.5348417	0.335587722	0.181571319
PCSK1N	−2.75543613	6.15*E* − 05	0.03089422	0.8535132	0.306834536	0.041926028
RAD23A	−1.486686178	1.19*E* − 05	−0.06985249	0.4657511	0.155919127	0.023202481
RPH3A	−2.205389128	0.000121979	−0.13636354	0.5549691	0.421580071	0.13750631
SLC17A6	−1.830552051	0.001580552	−0.03324685	0.816987	0.464266073	0.117376592
SYN1	−2.299673462	1.58*E* − 05	0.02889328	0.9464393	0.452666293	0.078849751
TOMM40	−0.736830295	0.015992849	0.30903301	0.4934736	0.146321059	0.022047574
TUBB4B	−2.679987878	0.000319179	0.07067393	0.4499649	0.276553902	0.062125723

(Continued)

TABLE 5 | Continued

Up-regulated	log2FoldChange	*P*-Value	log2FoldChange	*P*-Value	log2FoldChange	*P*-Value
ADAP2	0.51283287	0.118857833	-0.06659797	0.8099246	0.226833787	0.23714665
APBB1IP	0.587584434	0.084938225	−0.00896342	0.9812134	−0.079441481	0.661738945
ARFGAP3	1.236283159	0.023286482	0.09021196	0.4114407	−0.035664345	0.74369762
ATRAID	0.625394024	0.316212	0.23423602	0.1543085	−0.044280464	0.76558655
B2M	1.447935973	0.076662517	−0.34208579	0.2037221	−0.041599563	0.71977472
CAPN2	0.84824728	0.053265641	0.17151879	0.2941073	−0.213466413	0.179983124
CLU	0.478529519	0.322071446	−0.2573437	0.0879138	−0.024910105	0.955459054
CP	0.709886275	0.181039467	−0.78974274	0.1119182	0.101947077	0.871136325
DYNLT1	0.818264314	0.079915503	0.05107443	0.725406	−0.020183755	0.897716773
FAM133B	0.778470534	0.051976016	−0.21216533	0.0908713	−0.247661748	0.019678966
GFAP	0.800783703	0.036506933	−0.21606756	0.5421759	−0.00386905	0.989972713
HSPB8	0.496766253	0.077107061	0.04498535	0.8190471	−0.077219912	0.830926271
IGSF6	0.501189469	0.262839015	−0.27632074	0.4853182	−0.067940231	0.758869601
IQCK	0.333964298	0.13445688	−0.11592661	0.371691	−0.061655779	0.581519573
LAP3	0.897642777	0.145483073	−0.24390316	0.2506934	0.010833758	0.940660335
MAN2A1	0.747002323	0.172935628	−0.14157596	0.5729284	−0.682271726	0.054038553
MEGF10	0.556993686	0.116067563	−0.11060319	0.5623855	−0.336183288	0.089069161
NPL	0.446722265	0.131361543	0.00311247	0.9926684	−0.078551165	0.757780969
PLXDC2	0.508542748	0.14792643	−0.2940696	0.2734916	−0.234337594	0.176238219
PRDX1	0.766030612	0.301038221	−0.10469149	0.3129033	0.000517866	0.995942177
PRDX6	0.760314179	0.091473535	−0.08819497	0.5972124	−0.028179809	0.882624237
RAB10	0.442205285	0.105401194	−0.00327892	0.9775461	−0.021016368	0.747519625
SERPINA3	1.778045885	0.153542154	−0.7074398	0.3106779	0.53138378	0.379307158
SLC16A9	−0.083397868	0.891622356	−0.01895744	0.9275386	−0.133889726	0.776238048
SRSF6	0.589149827	0.172326071	0.00669309	0.943216	0.126191487	0.600178046
TAC1	1.995303687	0.202041997	0.19367133	0.5835214	−0.523156572	0.688917746
WDR11	0.811309106	0.060864791	0.13336214	0.3471851	−0.35430392	0.019054577

Down-regulated	Medial temporal gyrus(MTG)			
	GSE5281		GSE84422	
	log2FoldChange	*P*-Value	log2FoldChange	*P*-Value
MT3	0.471971901	0.06961523	0.006264733	0.376461879
SEPP1	0.952243496	0.049773528	0.025532798	0.310596068
NME2	0.253272544	0.295414163	0.007540923	0.012257472
EEF2	0.450031233	0.0824617	0.000633239	0.600645423

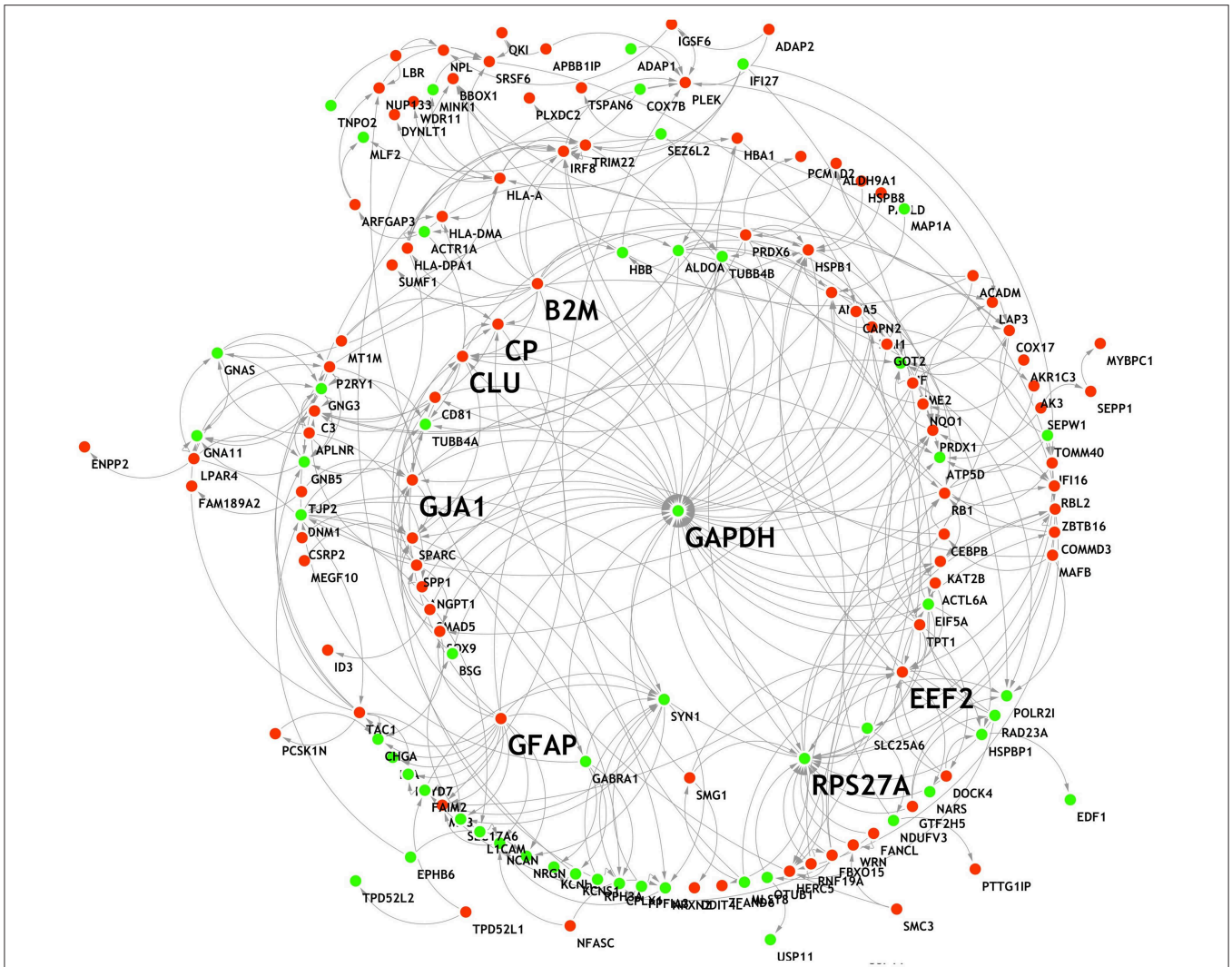

FIGURE 5 | PPI network of the DEGs. Red, up-regulation; green, down-regulation.

The Transcription Factors Associated With the AD-Associated/Other Neurodegenerative Disease-Associated DEGs and miRNAs

By analyzing TF–gene regulation, we found 442 gene-associated TFs (gTFs) associated with 55 AD-associated DEGs (**Table S8**), and 400 gTFs associated with 42 other neurodegenerative disease-associated DEGs (**Table S9**).

By studying the regulatory relationships between TFs and miRNAs, we obtained 253 miRNA-associated TFs (mTFs) associated with 50 AD-associated miRNAs (**Table S10**), and 118 mTFs associated with 22 other neurodegenerative disease-associated miRNAs whose target genes were identified as AD-associated DEGs in our study (**Table S11**).

mTF–miRNA–gene–gTF Regulatory Network

A regulatory network was constructed to study the regulatory interactions further, containing the AD-associated DEGs, the TFs associated with these genes (gTFs), the AD-associated miRNAs associated with these genes, the other neurodegenerative disease-associated miRNAs targeting these DEGs, and the TFs related to these miRNAs (mTFs). To study the other neurodegenerative disease-associated DEGs further, the TFs associated with these genes (gTFs), the AD-associated miRNAs targeting these genes, and the TFs related to these miRNAs (mTFs) were also analyzed.

This showed that *NFASC* and *ADAP1* are regulated by the most gTFs, 114 and 111, respectively. *NFASC* is involved in multiple sclerosis (Kawamura, 2014), and *ADAP1* is involved

TABLE 6 | The hub genes identified from the meta-analysis DEGs.

Gene symbols	Degree	ClosenessCentrality	Meta.expression	Meta. Qpval	Meta. pval	Brain tissue
GAPDH	39	0.47727273	−0.543132906	0.903040583	0.011108607	EC
RPS27A	25	0.42241379	−0.506389968	0.501831808	0.00902696	HIP
B2M	13	0.3878628	0.353023046	0.579830231	0.040853160	EC
GFAP	16	0.38582677	0.398018735	0.353484653	0.013506136	EC
EEF2	14	0.3828125	0.386796708	0.358680034	0.043927779	MTG
CP	10	0.38582677	0.523351329	0.918943259	0.0137236	EC
CLU	12	0.38481675	0.447778971	0.448785848	0.01315427	EC
GJA1	10	0.3828125	0.252228568	0.674305099	0.045547895	HIP

in AD (Stricker and Reiser, 2014). We also found gTFs for the hub genes Glyceraldehyde-3-phosphate dehydrogenase (*GAPDH*), ribosomal protein S27a *(RPS27A*), Glial fibrillary acidic protein (*GFAP)*, Beta-2 microglobulin (*B2M)*, Clusterin (*CLU)*, Eukaryotic elongation factor 2 (*EEF2)*, Gap junction protein alpha 1 (*GJA1),* and Ceruloplasmin (*CP*).

RAB10 and *TUBB4B* are regulated by the most miRNAs, 25 and 16, respectively. Both genes have been reported to be associated with AD (Olah et al., 2011; Martins-de-Souza et al., 2012).

Analysis of the regulatory network identified the presence of 131 interesting feed-forward loops (FFLs) (**Table S12**), in which a TF controls a miRNA and together they coregulate a target gene. These 131 FFLs involved 22 DEGs (20 AD-associated DEGs and two other neurodegenerative disease-associated DEGs), 31 miRNAs (26 AD-associated miRNAs and five other neurodegenerative disease-associated miRNAs), and 28 TFs. It was interesting that an FFL was identified between the gene *SERPINA3*, hsa-miR-27a, and the TF MYC, shown in **Figure 6**. Interestingly, our study found that two other neurodegenerative disease-associated DEGs are involved in such FFLs between the gene *STARD7*, hsa-miR-433, and the TF SMAD3, the gene *STARD7*, hsa-miR-31, and the TF SMAD3, the gene *TRIM22*, hsa-miR-31, and the TF ELK1, the gene *TRIM22*, hsa-miR-31, and the TF SMAD3, and the gene *TRIM22*, hsa-miR-31, and the TF SOX4. Hsa-miR-433 and hsa-miR-31 have already been reported to be associated with AD. Therefore, the associations between AD and the genes *STARD7* and *TRIM22* were studied further.

Verification of FFL Between the Gene SERPINA3, hsa-miR-27a, and TF MYC

GEO dataset (GSE16759) studying mRNA and miRNA was analyzed. This result revealed that SERPINA3 and MYC are upregulated, and hsa-miR-27a is downregulated in AD patients compared with controls. Detailed information is shown in **Table 11**.

To further verify the results, GSE46579 dataset studying miRNA expression in AD patients and controls blood was analyzed. Hsa-miR-27a was shown downregulated in AD patients blood. GSE97760 dataset studying mRNA expression was analyzed. The expression of SERPINA3 was shown upregulated, however MYC was shown downregulated. Detailed information is shown in **Table 11**.

SNP Analysis of the AD-Associated DEGs

SNPs corresponding to the AD-associated DEGs were obtained from the MirSNP online database. This showed that 1051 miRNAs were related to these SNPs, of which 79 miRNAs were AD associated. The results showed that 173 SNPs were related to these 79 miRNAs, and these 173 SNPs were associated with 40 AD-associated DEGs identified in our study. The chromosome loci information of these 173 SNPs is shown in **Table S13**.

DISCUSSION

In the past decades, research on the progression of AD has been productive, however identification of more potential genes and pathways in the pathogenesis of AD is needed. Therefore, large sample studies are essential for studying the effects of genes on the development of AD, and meta-analysis allows new biological insights.

In this study, we obtained DEGs by meta-analysis merging several AD-related microarray gene expression studies. This resulted in eight hubs with high degree and closeness centrality values, which are *GAPDH*, *RPS27A*, *GFAP*, *B2M*, *CLU*, *EEF2*, *GJA1,* and *CP*.

GAPDH co-localizes with most neurofibrillary tangles in the AD brain, and co-immunoprecipitates with abnormal tau antibodies in AD (Wang et al., 2005). The expression level of *GAPDH* in blood samples from familial AD patients is decreased compared with healthy controls (El Kadmiri et al., 2014).

RPS27A, a component of the 40S subunit of the ribosome, are associated with AD (Soler-Lopez et al., 2011).

GFAP, an astrocyte-specific intermediate filament, is significantly increased in AD mouse models compared with wildtype mice (Kamphuis et al., 2012).

B2M is the light chain of the first major histocompatibility (MHC) antigen. Increased plasma B2M results in deposition of amyloid fibrils, which is associated with over 20 degenerative diseases, including AD (Kardos et al., 2004).

CLU protein, an apolipoprotein, is responsible for clearing amyloid peptide and has neuroprotective effects for AD (Karch and Goate, 2015).

EEF2 is significantly decreased in AD compared with controls (Li et al., 2005).

TABLE 7 | AD-associate miRNAs associated with the AD-associate DEGs.

AD-associate DEGs	AD-associate miRNAs associated with genes	lncRNAs associated with miRNAs
ADAP1 (downregulated)	hsa-miR-21-3p	XLOC_013174
	hsa-miR-27a-5p	
BRSK2 (downregulated)	hsa-miR-27a-3p	C1orf132;DLX6-AS1;FLJ37201;IPW;KCNA3;KCNQ1OT1;LINC00548;LINC00662;LOC283070;MIR4534;NEAT1;RASSF8-AS1;RP11-111K18.2;RP11-129M16.4;RP11-175O19.4;RP11-196G18.22;RP11-314B1.2;RP11-361F15.2;RP11-553L6.5;RP11-94L15.2;RP13-735L24.1;RPA3-AS1;SNHG14;TMX2-CTNND1;TOB1-AS1;XLOC_003240;XLOC_008152;XLOC_010463;XLOC_011185;XLOC_013093;XXbac-BPGBPG55C20.2
DMTN (downregulated)	hsa-miR-124-3p	AL022344.7;ERVK13-1;KCNQ1OT1;LINC00643;LOC284581;NEAT1;RAD51L3-RFFL;RP11-508N22.12;RP11-731J8.2;RP11-74E22.8;TMEM256-PLSCR3;TTTY15;XLOC_006753;XLOC_010853;XLOC_013174;XLOC_013844
	hsa-miR-27a-3p	C1orf132;DLX6-AS1;FLJ37201;IPW;KCNA3;KCNQ1OT1;LINC00548;LINC00662;LOC283070;MIR4534;NEAT1;RASSF8-AS1;RP11-111K18.2;RP11-129M16.4;RP11-175O19.4;RP11-196G18.22;RP11-314B1.2;RP11-361F15.2;RP11-553L6.5;RP11-94L15.2;RP13-735L24.1;RPA3-AS1;SNHG14;TMX2-CTNND1;TOB1-AS1;XLOC_003240;XLOC_008152;XLOC_010463;XLOC_011185;XLOC_013093;XXbac-BPGBPG55C20.2
DNM1 (downregulated)	hsa-miR-124-3p	AL022344.7;ERVK13-1;KCNQ1OT1;LINC00643;LOC284581;NEAT1;RAD51L3-RFFL;RP11-508N22.12;RP11-731J8.2;RP11-74E22.8;TMEM256-PLSCR3;TTTY15;XLOC_006753;XLOC_010853;XLOC_013174;XLOC_013844
	hsa-miR-128-3p	
	hsa-miR-27a-3p	C1orf132;DLX6-AS1;FLJ37201;IPW;KCNA3;KCNQ1OT1;LINC00548;LINC00662;LOC283070;MIR4534;NEAT1;RASSF8-AS1;RP11-111K18.2;RP11-129M16.4;RP11-175O19.4;RP11-196G18.22;RP11-314B1.2;RP11-361F15.2;RP11-553L6.5;RP11-94L15.2;RP13-735L24.1;RPA3-AS1;SNHG14;TMX2-CTNND1;TOB1-AS1;XLOC_003240;XLOC_008152;XLOC_010463;XLOC_011185;XLOC_013093;XXbac-BPGBPG55C20.2
	hsa-miR-9-5p	CTB-89H12.4;KCNQ1OT1;RP11-273G15.2;RP11-793H13.8;SNHG14;TSNAX-DISC1;TUG1;XLOC_013093
GNAS (downregulated)	hsa-miR-182-5p	HOXA10-HOXA9;KCNQ1OT1;PCAT19;RP1-309I22.2
	hsa-miR-424-5p	AC005540.3;C1orf132;C1RL-AS1;INO80B-WBP1;KCNQ1OT1;LINC00662;MIA-RAB4B;RP11-379I19.1;RP1-309I22.2;RP5-991G20.1;RP6-24A23.7;XIST;XLOC_006753;XLOC_008207
GNB5 (downregulated)	hsa-miR-124-3p	AL022344.7;ERVK13-1;KCNQ1OT1;LINC00643;LOC284581;NEAT1;RAD51L3-RFFL;RP11-508N22.12;RP11-731J8.2;RP11-74E22.8;TMEM256-PLSCR3;TTTY15;XLOC_006753;XLOC_010853;XLOC_013174;XLOC_013844
	hsa-miR-148b-3p	CASC7;OIP5-AS1;SLMO2-ATP5E;SNHG14
	hsa-miR-503-5p	
HCFC1R1 (downregulated)	hsa-miR-124-3p	AL022344.7;ERVK13-1;KCNQ1OT1;LINC00643;LOC284581;NEAT1;RAD51L3-RFFL;RP11-508N22.12;RP11-731J8.2;RP11-74E22.8;TMEM256-PLSCR3;TTTY15;XLOC_006753;XLOC_010853;XLOC_013174;XLOC_013844
	hsa-miR-23b-3p	CASC7;CTC-459F4.3;KCNQ1OT1;NEAT1;RP11-159G9.5;RP11-215G15.5;SNHG14;TOB1-AS1;XIST;XLOC_005784;ZNRD1-AS1
	hsa-miR-27a-5p	
HSPBP1 (downregulated)	hsa-miR-27a-3p	C1orf132;DLX6-AS1;FLJ37201;IPW;KCNA3;KCNQ1OT1;LINC00548;LINC00662;LOC283070;MIR4534;NEAT1;RASSF8-AS1;RP11-111K18.2;RP11-129M16.4;RP11-175O19.4;RP11-196G18.22;RP11-314B1.2;RP11-361F15.2;RP11-553L6.5;RP11-94L15.2;RP13-735L24.1;RPA3-AS1;SNHG14;TMX2-CTNND1;TOB1-AS1;XLOC_003240;XLOC_008152;XLOC_010463;XLOC_011185;XLOC_013093;XXbac-BPGBPG55C20.2
INA (downregulated)	hsa-let-7b-5p	AP001055.6;BACE1-AS;CASC7;HOXA10-HOXA9;KCNQ1OT1;NEAT1;RP11-23J9.4;RP11-391M1.4;RP11-438B23.2;RP11-834C11.4;RP11-923I11.8;ST3GAL5-AS1;TRG-AS1;TUG1;XIST;XLOC_000647
	hsa-miR-16-5p	AC005540.3;FGF14-IT1;GS1-358P8.4;LINC00662;RP11-359B12.2;RP11-361F15.2;RP11-96D1.10;RP3-508I15.20;RP6-24A23.7;XLOC_003546;XLOC_006753;XLOC_008207;XLOC_013174
L1CAM (downregulated)	hsa-let-7b-5p	AP001055.6;BACE1-AS;CASC7;HOXA10-HOXA9;KCNQ1OT1;NEAT1;RP11-23J9.4;RP11-391M1.4;RP11-438B23.2;RP11-834C11.4;RP11-923I11.8;ST3GAL5-AS1;TRG-AS1;TUG1;XIST;XLOC_000647
	hsa-miR-124-3p	AL022344.7;ERVK13-1;KCNQ1OT1;LINC00643;LOC284581;NEAT1;RAD51L3-RFFL;RP11-508N22.12;RP11-731J8.2;RP11-74E22.8;TMEM256-PLSCR3;TTTY15;XLOC_006753;XLOC_010853;XLOC_013174;XLOC_013844
	hsa-miR-16-5p	AC005540.3;FGF14-IT1;GS1-358P8.4;LINC00662;RP11-359B12.2;RP11-361F15.2;RP11-96D1.10;RP3-508I15.20;RP6-24A23.7;XLOC_003546;XLOC_006753;XLOC_008207;XLOC_013174
	hsa-miR-182-5p	HOXA10-HOXA9;KCNQ1OT1;PCAT19;RP1-309I22.2
	hsa-miR-195-5p	AC005540.3;FGF14-IT1;GS1-358P8.4;KCNQ1OT1;LINC00662;RP11-361F15.2;RP11-96D1.10;RP5-991G20.1;RP6-24A23.7;XLOC_006753;XLOC_008207;XLOC_013174
	hsa-miR-375	KCNQ1OT1;SNHG14;SNORD116-20

(Continued)

TABLE 7 | Continued

AD-associate DEGs	AD-associate miRNAs associated with genes	lncRNAs associated with miRNAs
MLST8 (downregulated)	hsa-let-7b-5p	AP001055.6;BACE1-AS;CASC7;HOXA10-HOXA9;KCNQ1OT1;NEAT1;RP11-23J9.4;RP11-391M1.4;RP11-438B23.2;RP11-834C11.4;RP11-923I11.8;ST3GAL5-AS1;TRG-AS1;TUG1;XIST;XLOC_000647
	hsa-miR-124-3p	AL022344.7;ERVK13-1;KCNQ1OT1;LINC00643;LOC284581;NEAT1;RAD51L3-RFFL;RP11-508N22.12;RP11-731J8.2;RP11-74E22.8;TMEM256-PLSCR3;TTTY15;XLOC_006753;XLOC_010853;XLOC_013174;XLOC_013844
	hsa-miR-130a-3p	CASC7;H19;SNHG14
	hsa-miR-200b-3p	CTC-444N24.11;XIST;XLOC_013174
NDUFV3 (downregulated)	hsa-let-7a-5p	AP001055.6;BACE1-AS;CASC7;HOXA10-HOXA9;KCNQ1OT1;MEG3;NEAT1;RP11-391M1.4;RP11-438B23.2;RP11-834C11.4;RP11-923I11.8;ST3GAL5-AS1;TRG-AS1;TUG1;XIST;XLOC_008829;XLOC_010445;XLOC_013274;ZNRD1-AS1
	hsa-let-7b-5p	AP001055.6;BACE1-AS;CASC7;HOXA10-HOXA9;KCNQ1OT1;NEAT1;RP11-23J9.4;RP11-391M1.4;RP11-438B23.2;RP11-834C11.4;RP11-923I11.8;ST3GAL5-AS1;TRG-AS1;TUG1;XIST;XLOC_000647
	hsa-let-7c-5p	CASC7;TRG-AS1;XIST;XLOC_010445
NRGN (downregulated)	hsa-miR-107	CASC7;KCNQ1OT1;LINC00662;MIR4534;RP11-361F15.2;RP6-24A23.7;STAG3L5P-PVRIG2P-PILRB;XLOC_006753
	hsa-miR-195-5p	AC005540.3;FGF14-IT1;GS1-358P8.4;KCNQ1OT1;LINC00662;RP11-361F15.2;RP11-96D1.10;RP5-991G20.1;RP6-24A23.7;XLOC_006753;XLOC_008207;XLOC_013174
	hsa-miR-26a-5p	CTD-3064H18.1;DLX6-AS1;GAS5;GS1-124K5.3;KCNQ1OT1;MIR181A1HG;RP11-1006G14.4;RP11-119F7.5;RP11-120E11.2;RP11-1C8.7;RP11-282O18.3;RP11-305E6.4;RP11-78O7.2;RP4-635E18.8;RP5-1172N10.4;THUMPD3-AS1;TUG1;VSTM2A-OT1;XLOC_001148;XLOC_002746;XLOC_013174
PCSK1N (downregulated)	hsa-miR-124-3p	AL022344.7;ERVK13-1;KCNQ1OT1;LINC00643;LOC284581;NEAT1;RAD51L3-RFFL;RP11-508N22.12;RP11-731J8.2;RP11-74E22.8;TMEM256-PLSCR3;TTTY15;XLOC_006753;XLOC_010853;XLOC_013174;XLOC_013844
RAD23A (downregulated)	hsa-miR-124-3p	AL022344.7;ERVK13-1;KCNQ1OT1;LINC00643;LOC284581;NEAT1;RAD51L3-RFFL;RP11-508N22.12;RP11-731J8.2;RP11-74E22.8;TMEM256-PLSCR3;TTTY15;XLOC_006753;XLOC_010853;XLOC_013174;XLOC_013844
	hsa-miR-200b-3p	CTC-444N24.11;XIST;XLOC_013174
RPH3A (downregulated)	hsa-miR-27a-3p	C1orf132;DLX6-AS1;FLJ37201;IPW;KCNA3;KCNQ1OT1;LINC00548;LINC00662;LOC283070;MIR4534;NEAT1;RASSF8-AS1;RP11-111K18.2;RP11-129M16.4;RP11-175O19.4;RP11-196G18.22;RP11-314B1.2;RP11-361F15.2;RP11-553L6.5;RP11-94L15.2;RP13-735L24.1;RPA3-AS1;SNHG14;TMX2-CTNND1;TOB1-AS1;XLOC_003240;XLOC_008152;XLOC_010463;XLOC_011185;XLOC_013093;XXbac-BPGBPG55C20.2
RPS27A (downregulated)	hsa-miR-181a-5p	AC000403.4;CASC7;CTB-89H12.4;IPW;KCNIP4-IT1;KCNQ1OT1;LINC00506;N4BP2L2-IT2;RP11-10E18.7;RP11-1134I14.8;RP11-147L13.14;RP11-314B1.2;RP11-361F15.2;RP11-707A18.1;RP1-309I22.2;XLOC_003971;XLOC_010463;XLOC_011185;ZNF883;ZNRD1-AS1
SLC17A6 (downregulated)	hsa-miR-27a-3p	C1orf132;DLX6-AS1;FLJ37201;IPW;KCNA3;KCNQ1OT1;LINC00548;LINC00662;LOC283070;MIR4534;NEAT1;RASSF8-AS1;RP11-111K18.2;RP11-129M16.4;RP11-175O19.4;RP11-196G18.22;RP11-314B1.2;RP11-361F15.2;RP11-553L6.5;RP11-94L15.2;RP13-735L24.1;RPA3-AS1;SNHG14;TMX2-CTNND1;TOB1-AS1;XLOC_003240;XLOC_008152;XLOC_010463;XLOC_011185;XLOC_013093;XXbac-BPGBPG55C20.2
TOMM40 (downregulated)	hsa-miR-124-3p	AL022344.7;ERVK13-1;KCNQ1OT1;LINC00643;LOC284581;NEAT1;RAD51L3-RFFL;RP11-508N22.12;RP11-731J8.2;RP11-74E22.8;TMEM256-PLSCR3;TTTY15;XLOC_006753;XLOC_010853;XLOC_013174;XLOC_013844
TUBB4B (downregulated)	hsa-let-7b-5p	AP001055.6;BACE1-AS;CASC7;HOXA10-HOXA9;KCNQ1OT1;NEAT1;RP11-23J9.4;RP11-391M1.4;RP11-438B23.2;RP11-834C11.4;RP11-923I11.8;ST3GAL5-AS1;TRG-AS1;TUG1;XIST;XLOC_000647
	hsa-miR-128-3p	
	hsa-miR-148b-3p	CASC7;CTD-2303H24.2;OIP5-AS1;SLMO2-ATP5E;SNHG14
	hsa-miR-16-5p	AC005540.3;FGF14-IT1;GS1-358P8.4;KCNQ1OT1;LINC00662;RP11-359B12.2;RP11-361F15.2;RP11-96D1.10;RP3-508I15.20;RP6-24A23.7;XLOC_003546;XLOC_006753;XLOC_008207;XLOC_013174
	hsa-miR-17-5p	AC006548.28;CTB-89H12.4;CTD-2015H6.3;GABPB1-AS1;HCG11;LINC00657;MIR6080;MIR8072;PWAR6;PWARSN;RP11-162A12.4;RP11-171I2.1;RP11-361F15.2;RP11-363E7.4;RP11-399O19.9;RP11-553L6.5;RP11-81A1.6;RP11-909M7.3;XLOC_011677
	hsa-miR-18a-5p	AC000403.4;CASC7;CTB-89H12.4;IPW;KCNIP4-IT1;KCNQ1OT1;LINC00506;N4BP2L2-IT2;RP11-10E18.7;RP11-1134I14.8;RP11-147L13.14;RP11-314B1.2;RP11-361F15.2;RP11-707A18.1;RP1-309I22.2;XLOC_003971;XLOC_010463;XLOC_011185;ZNF883;ZNRD1-AS1

(Continued)

TABLE 7 | Continued

AD-associate DEGs	AD-associate miRNAs associated with genes	lncRNAs associated with miRNAs
	hsa-miR-18b-5p	XIST;XLOC_014102
	hsa-miR-23a-3p	CASC7;KCNQ1OT1;NEAT1;RP11-159G9.5;RP11-215G15.5;SNHG14;TOB1-AS1;XIST;ZNRD1-AS1
	hsa-miR-23b-3p	CASC7;CTC-459F4.3;KCNQ1OT1;NEAT1;RP11-159G9.5;RP11-215G15.5;SNHG14;TOB1-AS1;XIST;XLOC_005784;ZNRD1-AS1
	hsa-miR-27b-3p	C1orf132;DLX6-AS1;FLJ37201;IPW;KCNA3;KCNQ1OT1;LINC00548;LINC00662;LOC283070;NEAT1;RASSF8-AS1;RP11-111K18.2;RP11-129M16.4;RP11-175O19.4;RP11-196G18.22;RP11-314B1.2;RP11-553L6.5;RP11-94L15.2;RP13-735L24.1;RPA3-AS1;SNHG14;
ADAP2 (upregulated)	hsa-miR-16-5p	AC005540.3;FGF14-IT1;GS1-358P8.4;KCNQ1OT1;LINC00662;RP11-359B12.2;RP11-361F15.2;RP11-96D1.10;RP3-508I15.20;RP6-24A23.7;XLOC_003546;XLOC_006753;XLOC_008207;XLOC_013174
	hsa-miR-29c-3p	AC005154.6;AC006548.28;H19;KCNQ1OT1;LINC00674;MIR4697HG;NEAT1;RP11-314B1.2;RP11-582E3.6;RP4-630A11.3;THUMPD3-AS1;TTTY15;TUG1;XLOC_004366;XLOC_007942;XLOC_008295
	hsa-let-7b-5p	AP001055.6;BACE1-AS;CASC7;HOXA10-HOXA9;KCNQ1OT1;NEAT1;RP11-23J9.4;RP11-391M1.4;RP11-438B23.2;RP11-834C11.4;RP11-923I11.8;ST3GAL5-AS1;TRG-AS1;TUG1;XIST;XLOC_000647
	hsa-miR-101-3p	AC005235.1;CTD-2303H24.2;CTD-2571L23.8;FAM201A;HCG11;KCNQ1OT1;LINC00657;LINC00662;LINC00936;RP11-102L12.2;RP11-1134I14.8;RP11-196G18.24;RP11-350F4.2;RP11-378J18.8;RP11-421E14.2;XIST;XLOC_002872
APBB1IP (upregulated)	hsa-miR-27a-3p	C1orf132;DLX6-AS1;FLJ37201;IPW;KCNA3;KCNQ1OT1;LINC00548;LINC00662;LOC283070;MIR4534;NEAT1;RASSF8-AS1;RP11-111K18.2;RP11-129M16.4;RP11-175O19.4;RP11-196G18.22;RP11-314B1.2;RP11-361F15.2;RP11-553L6.5;RP11-94L15.2;RP13-735L24.1;RPA3-AS1;SNHG14;TMX2-CTNND1;TOB1-AS1;XLOC_003240;XLOC_008152;XLOC_010463;XLOC_011185;XLOC_013093;XXbac-BPGBPG55C20.2
ARFGAP3 (upregulated)	hsa-miR-200b-3p	CTC-444N24.11;XIST;XLOC_013174
ATRAID (upregulated)	hsa-miR-23b-3p	CASC7;CTC-459F4.3;KCNQ1OT1;NEAT1;RP11-159G9.5;RP11-215G15.5;SNHG14;TOB1-AS1;XIST;XLOC_005784;ZNRD1-AS1
	hsa-let-7b-5p	AP001055.6;BACE1-AS;CASC7;HOXA10-HOXA9;KCNQ1OT1;NEAT1;RP11-23J9.4;RP11-391M1.4;RP11-438B23.2;RP11-834C11.4;RP11-923I11.8;ST3GAL5-AS1;TRG-AS1;TUG1;XIST;XLOC_000647
	hsa-miR-101-3p	AC005235.1;CTD-2303H24.2;CTD-2571L23.8;FAM201A;HCG11;KCNQ1OT1;LINC00657;LINC00662;LINC00936;RP11-102L12.2;RP11-1134I14.8;RP11-196G18.24;RP11-350F4.2;RP11-378J18.8;RP11-421E14.2;XIST;XLOC_002872
	hsa-miR-16-5p	AC005540.3;FGF14-IT1;GS1-358P8.4;KCNQ1OT1;LINC00662;RP11-359B12.2;RP11-361F15.2;RP11-96D1.10;RP3-508I15.20;RP6-24A23.7;XLOC_003546;XLOC_006753;XLOC_008207;XLOC_013174
CAPN2 (upregulated)	hsa-miR-101-3p	AC005235.1;CTD-2303H24.2;CTD-2571L23.8;FAM201A;HCG11;KCNQ1OT1;LINC00657;LINC00662;LINC00936;RP11-102L12.2;RP11-1134I14.8;RP11-196G18.24;RP11-350F4.2;RP11-378J18.8;RP11-421E14.2;XIST;XLOC_002872
	hsa-miR-148b-3p	CASC7;CTD-2303H24.2;OIP5-AS1;SLMO2-ATP5E;SNHG14
	hsa-miR-124-3p	AL022344.7;ERVK13-1;KCNQ1OT1;LINC00643;LOC284581;NEAT1;RAD51L3-RFFL;RP11-508N22.12;RP11-731J8.2;RP11-74E22.8;TMEM256-PLSCR3;TTTY15;XLOC_006753;XLOC_010853;XLOC_013174;XLOC_013844
	hsa-miR-101-3p	AC005235.1;CTD-2303H24.2;CTD-2571L23.8;FAM201A;HCG11;KCNQ1OT1;LINC00657;LINC00662;LINC00936;RP11-102L12.2;RP11-1134I14.8;RP11-196G18.24;RP11-350F4.2;RP11-378J18.8;RP11-421E14.2;XIST;XLOC_002872
CP (upregulated)	hsa-miR-124-3p	AL022344.7;ERVK13-1;KCNQ1OT1;LINC00643;LOC284581;NEAT1;RAD51L3-RFFL;RP11-508N22.12;RP11-731J8.2;RP11-74E22.8;TMEM256-PLSCR3;TTTY15;XLOC_006753;XLOC_010853;XLOC_013174;XLOC_013844
	hsa-miR-182-5p	HOXA10-HOXA9;KCNQ1OT1;PCAT19;RP1-309I22.2
DYNLT1 (upregulated)	hsa-miR-23b-3p	CASC7;CTC-459F4.3;KCNQ1OT1;NEAT1;RP11-159G9.5;RP11-215G15.5;SNHG14;TOB1-AS1;XIST;XLOC_005784;ZNRD1-AS1
	hsa-miR-128-3p	
	hsa-miR-124-3p	AL022344.7;ERVK13-1;KCNQ1OT1;LINC00643;LOC284581;NEAT1;RAD51L3-RFFL;RP11-508N22.12;RP11-731J8.2;RP11-74E22.8;TMEM256-PLSCR3;TTTY15;XLOC_006753;XLOC_010853;XLOC_013174;XLOC_013844

(Continued)

TABLE 7 | Continued

AD-associate DEGs	AD-associate miRNAs associated with genes	lncRNAs associated with miRNAs
GFAP (upregulated)	hsa-miR-107	CASC7;KCNQ1OT1;LINC00662;MIR4534;RP11-361F15.2;RP6-24A23.7;STAG3L5P-PVRIG2P-PILRB;XLOC_006753
	hsa-miR-497-5p	AC005540.3;C1orf132;C1RL-AS1;FGF14-IT1;GS1-358P8.4;INO80B-WBP1;KCNQ1OT1;LINC00662;MIA-RAB4B;RP11-361F15.2;RP5-991G20.1;RP6-24A23.7;XIST;XLOC_006753;XLOC_008207;XLOC_013174;XLOC_013424
	hsa-miR-124-3p	AL022344.7;ERVK13-1;KCNQ1OT1;LINC00643;LOC284581;NEAT1;RAD51L3-RFFL;RP11-508N22.12;RP11-731J8.2;RP11-74E22.8;TMEM256-PLSCR3;TTTY15;XLOC_006753;XLOC_010853;XLOC_013174;XLOC_013844
	hsa-miR-15a-5p	AC005540.3;FGF14-IT1;GS1-358P8.4;KCNQ1OT1;LINC00662;MCM3AP-AS1;RP11-361F15.2;RP11-96D1.10;RP3-508I15.20;RP5-991G20.1;RP6-24A23.7;XLOC_003546;XLOC_008207;XLOC_006753;XLOC_013174
	hsa-miR-15b-5p	AC005540.3;FGF14-IT1;GS1-358P8.4;KCNQ1OT1;LINC00662;RP11-361F15.2;RP11-96D1.10;RP3-508I15.20;RP6-24A23.7;XLOC_008207;XLOC_013174
	hsa-miR-16-5p	AC005540.3;FGF14-IT1;GS1-358P8.4;KCNQ1OT1;LINC00662;RP11-359B12.2;RP11-361F15.2;RP11-96D1.10;RP3-508I15.20;RP6-24A23.7;XLOC_003546;XLOC_006753;XLOC_008207;XLOC_013174
	hsa-miR-195-5p	AC005540.3;FGF14-IT1;GS1-358P8.4;KCNQ1OT1;LINC00662;RP11-361F15.2;RP11-96D1.10;RP5-991G20.1;RP6-24A23.7;XLOC_006753;XLOC_008207;XLOC_013174
	hsa-miR-24-3p	CTA-292E10.9;CTC-273B12.8;GABPB1-AS1;LINC00662;LOC388692;MIR4534;RP11-54O7.1;XLOC_006242;XLOC_008461;XLOC_011313
HSPB8 (upregulated)	hsa-miR-124-3p	AL022344.7;ERVK13-1;KCNQ1OT1;LINC00643;LOC284581;NEAT1;RAD51L3-RFFL;RP11-508N22.12;RP11-731J8.2;RP11-74E22.8;TMEM256-PLSCR3;TTTY15;XLOC_006753;XLOC_010853;XLOC_013174;XLOC_013844
	hsa-let-7b-5p	AP001055.6;BACE1-AS;CASC7;HOXA10-HOXA9;KCNQ1OT1;NEAT1;RP11-23J9.4;RP11-391M1.4;RP11-438B23.2;RP11-834C11.4;RP11-923I11.8;ST3GAL5-AS1;TRG-AS1;TUG1;XIST;XLOC_000647
	hsa-miR-16-5p	AC005540.3;FGF14-IT1;GS1-358P8.4;KCNQ1OT1;LINC00662;RP11-359B12.2;RP11-361F15.2;RP11-96D1.10;RP3-508I15.20;RP6-24A23.7;XLOC_003546;XLOC_006753;XLOC_008207;XLOC_013174
	hsa-miR-133a-3p	
IQCK (upregulated)	hsa-miR-124-3p	AL022344.7;ERVK13-1;KCNQ1OT1;LINC00643;LOC284581;NEAT1;RAD51L3-RFFL;RP11-508N22.12;RP11-731J8.2;RP11-74E22.8;TMEM256-PLSCR3;TTTY15;XLOC_006753;XLOC_010853;XLOC_013174;XLOC_013844
	hsa-miR-107	CASC7;KCNQ1OT1;LINC00662;MIR4534;RP11-361F15.2;RP6-24A23.7;STAG3L5P-PVRIG2P-PILRB;XLOC_006753
LAP3 (upregulated)	hsa-miR-495-3p	
	hsa-miR-503-5p	
	hsa-miR-124-3p	AL022344.7;ERVK13-1;KCNQ1OT1;LINC00643;LOC284581;NEAT1;RAD51L3-RFFL;RP11-508N22.12;RP11-731J8.2;RP11-74E22.8;TMEM256-PLSCR3;TTTY15;XLOC_006753;XLOC_010853;XLOC_013174;XLOC_013844
	hsa-miR-128-3p	
	hsa-miR-16-5p	AC005540.3;FGF14-IT1;GS1-358P8.4;KCNQ1OT1;LINC00662;RP11-359B12.2;RP11-361F15.2;RP11-96D1.10;RP3-508I15.20;RP6-24A23.7;XLOC_003546;XLOC_006753;XLOC_008207;XLOC_013174
	hsa-miR-21-3p	XLOC_013174
	hsa-miR-27a-5p	
	hsa-miR-133a-3p	
MAN2A1 (upregulated)	hsa-miR-27a-3p	C1orf132;DLX6-AS1;FLJ37201;IPW;KCNA3;KCNQ1OT1;LINC00548;LINC00662;LOC283070;MIR4534;NEAT1;RASSF8-AS1;RP11-111K18.2;RP11-129M16.4;RP11-175O19.4;RP11-196G18.22;RP11-314B1.2;RP11-361F15.2;RP11-553L6.5;RP11-94L15.2;RP13-735L24.1;RPA3-AS1;SNHG14;TMX2-CTNND1;TOB1-AS1;XLOC_003240;XLOC_008152;XLOC_010463;XLOC_011185;XLOC_013093;XXbac-BPGBPG55C20.2
	hsa-miR-27b-3p	C1orf132;DLX6-AS1;FLJ37201;IPW;KCNA3;KCNQ1OT1;LINC00548;LINC00662;LOC283070;NEAT1;RASSF8-AS1;RP11-111K18.2;RP11-129M16.4;RP11-175O19.4;RP11-196G18.22;RP11-314B1.2;RP11-553L6.5;RP11-94L15.2;RP13-735L24.1;RPA3-AS1;SNHG14
	hsa-miR-124-3p	AL022344.7;ERVK13-1;KCNQ1OT1;LINC00643;LOC284581;NEAT1;RAD51L3-RFFL;RP11-508N22.12;RP11-731J8.2;RP11-74E22.8;TMEM256-PLSCR3;TTTY15;XLOC_006753;XLOC_010853;XLOC_013174;XLOC_013844
	hsa-let-7b-5p	AP001055.6;BACE1-AS;CASC7;HOXA10-HOXA9;KCNQ1OT1;NEAT1;RP11-23J9.4;RP11-391M1.4;RP11-438B23.2;RP11-834C11.4;RP11-923I11.8;ST3GAL5-AS1;TRG-AS1;TUG1;XIST;XLOC_000647

(Continued)

TABLE 7 | Continued

AD-associate DEGs	AD-associate miRNAs associated with genes	lncRNAs associated with miRNAs
	hsa-miR-182-5p	HOXA10-HOXA9;KCNQ1OT1;PCAT19;RP1-309I22.2
MEGF10 (upregulated)	hsa-miR-26a-5p	CTD-3064H18.1;DLX6-AS1;GAS5;GS1-124K5.3;KCNQ1OT1;MIR181A1HG;RP11-1006G14.4;RP11-119F7.5;RP11-120E11.2;RP11-1C8.7;RP11-282O18.3;RP11-305E6.4;RP11-78O7.2;RP4-635E18.8;RP5-1172N10.4;THUMPD3-AS1;TUG1;VSTM2A-OT1;XLOC_001148;XLOC_002746;XLOC_013174
	hsa-miR-101-3p	AC005235.1;CTD-2303H24.2;CTD-2571L23.8;FAM201A;HCG11;KCNQ1OT1;LINC00657;LINC00662;LINC00936;RP11-102L12.2;RP11-1134I14.8;RP11-196G18.24;RP11-350F4.2;RP11-378J18.8;RP11-421E14.2;XIST;XLOC_002872
	hsa-miR-182-5p	HOXA10-HOXA9;KCNQ1OT1;PCAT19;RP1-309I22.2
MT1M (upregulated)	hsa-miR-124-3p	AL022344.7;ERVK13-1;KCNQ1OT1;LINC00643;LOC284581;NEAT1;RAD51L3-RFFL;RP11-508N22.12;RP11-731J8.2;RP11-74E22.8;TMEM256-PLSCR3;TTTY15;XLOC_006753;XLOC_010853;XLOC_013174;XLOC_013844
	hsa-miR-21-3p	XLOC_013174
	hsa-miR-27a-3p	C1orf132;DLX6-AS1;FLJ37201;IPW;KCNA3;KCNQ1OT1;LINC00548;LINC00662;LOC283070;MIR4534;NEAT1;RASSF8-AS1;RP11-111K18.2;RP11-129M16.4;RP11-175O19.4;RP11-196G18.22;RP11-314B1.2;RP11-361F15.2;RP11-553L6.5;RP11-94L15.2;RP13-735L24.1;RPA3-AS1;SNHG14;TMX2-CTNND1;TOB1-AS1;XLOC_003240;XLOC_008152;XLOC_010463;XLOC_011185;XLOC_013093;XXbac-BPGBPG55C20.2
	hsa-miR-27a-5p	
	hsa-miR-376a-5p	KCNQ1OT1;SIK3-IT1
MT3 (upregulated)	hsa-let-7b-5p	AP001055.6;BACE1-AS;CASC7;HOXA10-HOXA9;KCNQ1OT1;NEAT1;RP11-23J9.4;RP11-391M1.4;RP11-438B23.2;RP11-834C11.4;RP11-923I11.8;ST3GAL5-AS1;TRG-AS1;TUG1;XIST;XLOC_000647
	hsa-miR-182-5p	HOXA10-HOXA9;KCNQ1OT1;PCAT19;RP1-309I22.2
NPL (upregulated)	hsa-miR-16-5p	AC005540.3;FGF14-IT1;GS1-358P8.4;KCNQ1OT1;LINC00662;RP11-359B12.2;RP11-361F15.2;RP11-96D1.10;RP3-508I15.20;RP6-24A23.7;XLOC_003546;XLOC_006753;XLOC_008207;XLOC_013174
	hsa-miR-27a-5p	
PCSK1N (upregulated)	hsa-miR-124-3p	AL022344.7;ERVK13-1;KCNQ1OT1;LINC00643;LOC284581;NEAT1;RAD51L3-RFFL;RP11-508N22.12;RP11-731J8.2;RP11-74E22.8;TMEM256-PLSCR3;TTTY15;XLOC_006753;XLOC_010853;XLOC_013174;XLOC_013844
PLXDC2 (upregulated)	hsa-miR-29a-3p	AC005154.6;AC006548.28;H19;KCNQ1OT1;LINC00674;MIR4697HG;NEAT1;RP11-314B1.2;RP11-582E3.6;RP4-630A11.3;THUMPD3-AS1;TTTY15;TUG1;XLOC_004366;XLOC_007942;XLOC_008295
	hsa-miR-29b-3p	AC005154.6;AC006548.28;H19;KCNQ1OT1;LINC00674;MIR4697HG;NEAT1;RP11-314B1.2;RP11-582E3.6;RP4-630A11.3;THUMPD3-AS1;TTTY15;TUG1;XLOC_004366;XLOC_007942;XLOC_008295
	hsa-miR-29c-3p	AC005154.6;AC006548.28;H19;KCNQ1OT1;LINC00674;MIR4697HG;NEAT1;RP11-314B1.2;RP11-582E3.6;RP4-630A11.3;THUMPD3-AS1;TTTY15;TUG1;XLOC_004366;XLOC_007942;XLOC_008295
	hsa-miR-27a-3p	AC005154.6;AC006548.28;H19;KCNQ1OT1;LINC00674;MIR4697HG;NEAT1;RP11-314B1.2;RP11-582E3.6;RP4-630A11.3;THUMPD3-AS1;TTTY15;TUG1;XLOC_004366;XLOC_007942;XLOC_008295
PRDX1 (upregulated)	hsa-miR-29a-3p	AC005154.6;AC006548.28;H19;KCNQ1OT1;LINC00674;MIR4697HG;NEAT1;RP11-314B1.2;RP11-582E3.6;RP4-630A11.3;THUMPD3-AS1;TTTY15;TUG1;XLOC_004366;XLOC_007942;XLOC_008295
	hsa-miR-23b-3p	CASC7;CTC-459F4.3;KCNQ1OT1;NEAT1;RP11-159G9.5;RP11-215G15.5;SNHG14;TOB1-AS1;XIST;XLOC_005784;ZNRD1-AS1
	hsa-miR-375	KCNQ1OT1;SNHG14;SNORD116-20
PRDX6 (upregulated)	hsa-miR-23b-3p	CASC7;CTC-459F4.3;KCNQ1OT1;NEAT1;RP11-159G9.5;RP11-215G15.5;SNHG14;TOB1-AS1;XIST;XLOC_005784;ZNRD1-AS1
	hsa-miR-124-3p	AL022344.7;ERVK13-1;KCNQ1OT1;LINC00643;LOC284581;NEAT1;RAD51L3-RFFL;RP11-508N22.12;RP11-731J8.2;RP11-74E22.8;TMEM256-PLSCR3;TTTY15;XLOC_006753;XLOC_010853;XLOC_013174;XLOC_013844
	hsa-miR-133a-3p	
RAB10 (upregulated)	hsa-miR-130b-3p	CASC7;H19;SNHG14
	hsa-miR-148b-3p	CASC7;CTD-2303H24.2;OIP5-AS1;SLMO2-ATP5E;SNHG14
	hsa-miR-107	CASC7;KCNQ1OT1;LINC00662;MIR4534;RP11-361F15.2;RP6-24A23.7;STAG3L5P-PVRIG2P-PILRB;XLOC_006753
	hsa-miR-16-5p;	AC005540.3;FGF14-IT1;GS1-358P8.4;KCNQ1OT1;LINC00662;RP11-359B12.2;RP11-361F15.2;RP11-96D1.10;RP3-508I15.20;RP6-24A23.7;XLOC_003546;XLOC_006753;XLOC_008207;XLOC_013174
	hsa-miR-124-3p	AL022344.7;ERVK13-1;KCNQ1OT1;LINC00643;LOC284581;NEAT1;RAD51L3-RFFL;RP11-508N22.12;RP11-731J8.2;RP11-74E22.8;TMEM256-PLSCR3;TTTY15;XLOC_006753;XLOC_010853;XLOC_013174;XLOC_013844

(Continued)

TABLE 7 | Continued

AD-associate DEGs	AD-associate miRNAs associated with genes	lncRNAs associated with miRNAs
	hsa-miR-15a-5p	AC005540.3;FGF14-IT1;GS1-358P8.4;KCNQ1OT1;LINC00662;MCM3AP-AS1;RP11-361F15.2;RP11-96D1.10;RP3-508I15.20;RP5-991G20.1;RP6-24A23.7;XLOC_003546;XLOC_008207;XLOC_006753;XLOC_013174
	hsa-miR-15b-5p	AC005540.3;FGF14-IT1;GS1-358P8.4;KCNQ1OT1;LINC00662;RP11-361F15.2;RP11-96D1.10;RP3-508I15.20;RP6-24A23.7;XLOC_008207;XLOC_013174
	hsa-miR-143-3p	AC090587.2;CTB-193M12.3;EEF1E1-BLOC1S5;FLJ31306;GABPB1-AS1;KCNQ1OT1;LINC00662;MESTIT1;OIP5-AS1;PDCD4-AS1;RP11-424G14.1;RP5-1014D13.2
	hsa-miR-30b-5p	AC096772.6;CASC7;CTA-292E10.9;CTB-89H12.4;HCG18;LINC00461;LOC100128288;MIA-RAB4B;OIP5-AS1;PWRN3;RP11-175O19.4;RP11-265E18.1;RP11-361F15.2;RP11-378J18.8;RP11-618G20.1;RP11-731J8.2;RP1-309I22.2;RP6-24A23.7;TRHDE-AS1;UG0898H09;XIST;XLOC_005753;XLOC_008207
	hsa-miR-30c-5p	AC096772.6;CASC7;CTA-292E10.9;CTB-89H12.4;LINC00461;LOC100128288;MIA-RAB4B;PWRN3;RP11-175O19.4;RP11-265E18.1;RP11-361F15.2;RP11-618G20.1;RP11-731J8.2;RP1-309I22.2;UG0898H09;XIST;XLOC_005753;XLOC_008207
	hsa-miR-195-5p	AC005540.3;FGF14-IT1;GS1-358P8.4;KCNQ1OT1;LINC00662;RP11-361F15.2;RP11-96D1.10;RP5-991G20.1;RP6-24A23.7;XLOC_006753;XLOC_008207;XLOC_013174
	hsa-miR-23a-3p	CASC7;KCNQ1OT1;NEAT1;RP11-159G9.5;RP11-215G15.5;SNHG14;TOB1-AS1;XIST;ZNRD1-AS1
	hsa-miR-23b-3p	CASC7;CTC-459F4.3;KCNQ1OT1;NEAT1;RP11-159G9.5;RP11-215G15.5;SNHG14;TOB1-AS1;XIST;XLOC_005784;ZNRD1-AS1
	hsa-miR-497-5p	AC005540.3;C1orf132;C1RL-AS1;FGF14-IT1;GS1-358P8.4;INO80B-WBP1;KCNQ1OT1;LINC00662;MIA-RAB4B;RP11-361F15.2;RP5-991G20.1;RP6-24A23.7;XIST;XLOC_006753;XLOC_008207;XLOC_013174;XLOC_013424
SEPP1 (upregulated)	hsa-miR-20a-5p	AC006548.28;CTB-89H12.4;LINC00116;GABPB1-AS1;RP11-553L6.5;RP11-81A1.6;SNORD109A;XIST;XLOC_002263;XLOC_004804;XLOC_013093
	hsa-miR-124-3p	AL022344.7;ERVK13-1;KCNQ1OT1;LINC00643;LOC284581;NEAT1;RAD51L3-RFFL;RP11-508N22.12;RP11-731J8.2;RP11-74E22.8;TMEM256-PLSCR3;TTTY15;XLOC_006753;XLOC_010853;XLOC_013174;XLOC_013844
	hsa-let-7b-5p	AP001055.6;BACE1-AS;CASC7;HOXA10-HOXA9;KCNQ1OT1;NEAT1;RP11-23J9.4;RP11-391M1.4;RP11-438B23.2;RP11-834C11.4;RP11-923I11.8;ST3GAL5-AS1;TRG-AS1;TUG1;XIST;XLOC_000647
	hsa-miR-101-3p	AC005235.1;CTD-2303H24.2;CTD-2571L23.8;FAM201A;HCG11;KCNQ1OT1;LINC00657;LINC00662;LINC00936;RP11-102L12.2;RP11-1134I14.8;RP11-196G18.24;RP11-350F4.2;RP11-378J18.8;RP11-421E14.2;XIST;XLOC_002872
	hsa-miR-128-3p	
	hsa-miR-26a-5p	CTD-3064H18.1;DLX6-AS1;GAS5;GS1-124K5.3;KCNQ1OT1;MIR181A1HG;RP11-1006G14.4;RP11-119F7.5;RP11-120E11.2;RP11-1C8.7;RP11-282O18.3;RP11-305E6.4;RP11-78O7.2;RP4-635E18.8;RP5-1172N10.4;THUMPD3-AS1;TUG1;VSTM2A-OT1;XLOC_001148;XLOC_002746;XLOC_013174
SERPINA3 (upregulated)	hsa-miR-124-3p	AL022344.7;ERVK13-1;KCNQ1OT1;LINC00643;LOC284581;NEAT1;RAD51L3-RFFL;RP11-508N22.12;RP11-731J8.2;RP11-74E22.8;TMEM256-PLSCR3;TTTY15;XLOC_006753;XLOC_010853;XLOC_013174;XLOC_013844
	hsa-miR-20a-5p	AC006548.28;CTB-89H12.4;LINC00116;GABPB1-AS1;RP11-553L6.5;RP11-81A1.6;SNORD109A;XIST;XLOC_002263;XLOC_004804;XLOC_013093
	hsa-miR-30d-5p	CASC7;CTA-292E10.9;CTB-89H12.4;HCG18;LINC00461;LOC100128288;RP11-175O19.4;RP11-361F15.2;RP11-618G20.1;RP1-309I22.2;RP6-24A23.7;XIST;XLOC_008207
	hsa-miR-130a-3p	CASC7;H19;SNHG14
	hsa-miR-182-5p	HOXA10-HOXA9;KCNQ1OT1;PCAT19;RP1-309I22.2
	hsa-miR-27a-3p	AC005154.6;AC006548.28;H19;KCNQ1OT1;LINC00674;MIR4697HG;NEAT1;RP11-314B1.2;RP11-582E3.6;RP4-630A11.3;THUMPD3-AS1;TTTY15;TUG1;XLOC_004366;XLOC_007942;XLOC_008295
SLC16A9 (upregulated)	hsa-miR-424-5p	AC005540.3;C1orf132;C1RL-AS1;INO80B-WBP1;KCNQ1OT1;LINC00662;MIA-RAB4B;RP11-379I19.1;RP1-309I22.2;RP5-991G20.1;RP6-24A23.7;XIST;XLOC_006753;XLOC_008207;
	hsa-miR-9-3p	ALMS1-IT1;ALMS1-IT1;RP11-175O19.4;RP11-438B23.2;RP4-714D9.5;TTN-AS1;XIST;XLOC_002872;XLOC_010463
	hsa-miR-101-3p	AC005235.1;CTD-2303H24.2;CTD-2571L23.8;FAM201A;HCG11;KCNQ1OT1;LINC00657;LINC00662;LINC00936;RP11-102L12.2;RP11-1134I14.8;RP11-196G18.24;RP11-350F4.2;RP11-378J18.8;RP11-421E14.2;XIST;XLOC_002872
	hsa-miR-21-3p	XLOC_013174
	hsa-miR-27a-5p	
	hsa-miR-29c-3p	AC005154.6;AC006548.28;H19;KCNQ1OT1;LINC00674;MIR4697HG;NEAT1;RP11-314B1.2;RP11-582E3.6;RP4-630A11.3;THUMPD3-AS1;TTTY15;TUG1;XLOC_004366;XLOC_007942;XLOC_008295

(Continued)

TABLE 7 | Continued

AD-associate DEGs	AD-associate miRNAs associated with genes	lncRNAs associated with miRNAs
SRSF6 (upregulated)	hsa-miR-26a-5p	CTD-3064H18.1;DLX6-AS1;GAS5;GS1-124K5.3;HOXA10-HOXA9;MIR181A1HG;MIR6080;RP11-1006G14.4;RP11-119F7.5;RP11-120E11.2;RP11-1C8.7;RP11-282O18.3;RP11-305E6.4;RP11-78O7.2;RP4-635E18.8;RP5-1172N10.4;THUMPD3-AS1;VSTM2A-OT1;XLOC_001148;XLOC_002746;XLOC_013174
	hsa-miR-93-5p	AC006548.28;CTB-89H12.4;CTD-2015H6.3;GABPB1-AS1;HCG11;LINC00657;MIR6080;MIR8072;PWAR6;PWARSN;RP11-162A12.4;RP11-361F15.2;RP11-363E7.4;RP11-399O19.9;RP11-553L6.5;RP11-909M7.3;XLOC_004804;XLOC_010706;XLOC_011677
	hsa-miR-340-5p	AC002429.5;CASC7;CTC-444N24.11;LINC00662;LINC01355;NEAT1;RP11-119F7.5;RP11-174G6.5;RP11-96D1.10;TUG1;XIST;XLOC_002282;XLOC_008207
	hsa-miR-137	CASC7;CTB-89H12.4;CTC-459F4.3;HCG18;KB-1410C5.5;OIP5-AS1;RP11-314B1.2;RP11-498C9.15;RP11-78O7.2;SNHG14;XLOC_004457
	hsa-miR-101-3p	AC005235.1;CTD-2303H24.2;CTD-2571L23.8;FAM201A;HCG11;KCNQ1OT1;LINC00657;LINC00662;LINC00936;RP11-102L12.2;RP11-1134I14.8;RP11-196G18.24;RP11-350F4.2;RP11-378J18.8;RP11-421E14.2;XIST;XLOC_002872
	hsa-miR-27a-3p	AC005154.6;AC006548.28;H19;KCNQ1OT1;LINC00674;MIR4697HG;NEAT1;RP11-314B1.2;RP11-582E3.6;RP4-630A11.3;THUMPD3-AS1;TTTY15;TUG1;XLOC_004366;XLOC_007942;XLOC_008295
	hsa-miR-27b-3p	C1orf132;DLX6-AS1;FLJ37201;IPW;KCNA3;KCNQ1OT1;LINC00548;LINC00662;LOC283070;NEAT1;RASSF8-AS1;RP11-111K18.2;RP11-129M16.4;RP11-175O19.4;RP11-196G18.22;RP11-314B1.2;RP11-553L6.5;RP11-94L15.2;RP13-735L24.1;RPA3-AS1;SNHG14;
	hsa-miR-124-3p	AL022344.7;ERVK13-1;KCNQ1OT1;LINC00643;LOC284581;NEAT1;RAD51L3-RFFL;RP11-508N22.12;RP11-731J8.2;RP11-74E22.8;TMEM256-PLSCR3;TTTY15;XLOC_006753;XLOC_010853;XLOC_013174;XLOC_013844
WDR11 (upregulated)	hsa-miR-26b-5p	GAS5;GS1-124K5.3;HOXA10-HOXA9;RP11-119F7.5;RP11-120E11.2;THUMPD3-AS1;TUG1;XLOC_013174
	hsa-miR-16-5p	AC005540.3;FGF14-IT1;GS1-358P8.4;KCNQ1OT1;LINC00662;RP11-359B12.2;RP11-361F15.2;RP3-508I15.20;RP6-24A23.7;XLOC_003546;XLOC_006753;XLOC_008207;XLOC_013174
	hsa-miR-182-5p	HOXA10-HOXA9;KCNQ1OT1;PCAT19;RP1-309I22.2
GJA1 (upregulated)	hsa-miR-107	CASC7;KCNQ1OT1;LINC00662;MIR4534;RP11-361F15.2;RP6-24A23.7;STAG3L5P-PVRIG2P-PILRB;XLOC_006753

GJA1, also known as connexin 43, shows upregulated mRNA and protein levels in AD (Ren et al., 2018). Specific deletion of astroglial connexin 43 in AD mice improved cognitive dysfunction (Ren et al., 2018).

CP, a ferrous oxidase enzyme, plays an important role in regulating iron metabolism and redox reactions. *CP* expression was significantly downregulated in the hippocampus region of AD patients, resulting in memory impairment and increased iron accumulation (Zhao et al., 2018).

However, the role of these genes in AD is not very clear. The importance of these genes requires further study in AD.

Studies also have shown that there is a difference between different sexes in neuroanatomy and function, so gender differences may be of great significance in the treatment of AD (Moradifard et al., 2018). More and more attention has been paid to the gender differences in AD prevalence. Some evidence showed that the risk of AD due to APOE ε4 allele is different in two sexes: female carriers are at higher risk of AD than male carriers (Nyarko et al., 2018). Based on our results, there are also a number of genes which specifically expressed in male and female. Such as CHC22 protein encoded by *CLTCL1* gene was strongly suggested to play important function in affecting neuronal progenitor cells or immature neurons, and *CLTCL1* was significantly upregulated in the development of human brain, especially cerebral cortex (Nahorski et al., 2015). LPIN1 plays a role in abdominal obesity, insulin sensitivity, and hypertriglyceridemia and it is associated to blood pressure regulation, especially in men (Ong et al., 2008). FOLR1 was reported to be overexpressed in ovarian cancer (Lin et al., 2013), and its expression could be regulated by both female sex hormones and retinoic acid (Kelemen et al., 2014). ELAVL2 might be critical for normal neuronal and synaptic function in the brain by regulating important genetic pathways participated in human neurodevelopment (Berto et al., 2016).

Analysis of FFL identified the bioregulatory relationship between the gene SERPINA3, hsa-miR-27a, and the TF MYC. TransmiR information revealed that hsa-miR-27a is repressed by the TF MYC. By combining the results of the DIANA-LncBase and TRANSFAC databases, both MYC and hsa-miR-27a were found to regulate the target gene *SERPINA3*. The expression of hsa-miR-27a is downregulated in AD patients compared with controls (Nunez-Iglesias et al., 2010), this result is also verified in our study and GSE46579 dataset (**Table 11**). MYC is also physiologically relevant and is increased in vulnerable neurons in patients with AD (Ferrer et al., 2001). This suggests that this TF may be highly expressed in the brain tissues of AD patients, indicating that MYC downregulates hsa-miR-27a. SERPINA3 is also involved in AD (Guan et al., 2012)

TABLE 8 | Other neurodegenerative disease-specific miRNAs associated with the AD-associate DEGs.

AD-associate DEGs	Other neurodegenerative disease-specific miRNAs associated with genes	lncRNAs associated with miRNAs
DMTN (downregulated)	hsa-miR-34a-5p	AC004951.6;AC092535.3;KCNQ1OT1;LINC00662;MIR4534;PCBP2-OT1;RP11-693J15.5
	hsa-miR-7-5p	AC005154.6;DLX6-AS1;KCNQ1OT1;LINC01233;LINC01314;MIR4534;OIP5-AS1;OIP5-AS1;RP11-679B19.1;RP1-309I22.2;XIST
FXYD7 (downregulated)	hsa-miR-212-3p	CASC7;CTB-89H12.4;NEAT1;RP11-26J3.3;XIST;XLOC_006753
GAPDH (downregulated)	hsa-miR-34a-5p	AC004951.6;AC092535.3;KCNQ1OT1;LINC00662;MIR4534;PCBP2-OT1;RP11-693J15.5
HSPBP1 (downregulated)	hsa-miR-194-5p	CTB-89H12.4;KCNQ1OT1
	hsa-miR-34a-5p	AC004951.6;AC092535.3;KCNQ1OT1;LINC00662;MIR4534;PCBP2-OT1;RP11-693J15.5
	hsa-miR-7-5p	AC005154.6;DLX6-AS1;KCNQ1OT1;LINC01233;LINC01314;MIR4534;OIP5-AS1;OIP5-AS1;RP11-679B19.1;RP1-309I22.2;XIST
INA (downregulated)	hsa-miR-212-3p	CASC7;CTB-89H12.4;NEAT1;RP11-26J3.3;XIST;XLOC_006753
	hsa-miR-34a-5p	AC004951.6;AC092535.3;KCNQ1OT1;LINC00662;MIR4534;PCBP2-OT1;RP11-693J15.5
MLST8 (downregulated)	hsa-miR-7-5p	AC005154.6;DLX6-AS1;KCNQ1OT1;LINC01233;LINC01314;MIR4534;OIP5-AS1;OIP5-AS1;RP11-679B19.1;RP1-309I22.2;XIST
NDUFV3 (downregulated)	hsa-miR-374a-5p	CTC-444N24.11;CTD-2561J22.5;RP11-613D13.5;TRG-AS1;XIST;XLOC_004545;XLOC_006322;ZNRD1-AS1
	hsa-miR-494-3p	
NRGN (downregulated)	hsa-miR-34a-5p	AC004951.6;AC092535.3;KCNQ1OT1;LINC00662;MIR4534;PCBP2-OT1;RP11-693J15.5
RPH3A (downregulated)	hsa-miR-136-3p	CTD-2140G10.2;KCNQ1OT1;LL22NC03-2H8.5;RP11-227G15.3;RP11-700J17.2;TTTY15;XLOC_008295
	hsa-miR-221-3p	AC000120.7;CTB-89H12.4;RP11-147L13.8
RPS27A (downregulated)	hsa-miR-485-3p	HCG11;LINC00657;RP11-482H16.1;RP11-95O2.1;RP3-445N2.1;XLOC_004244
SYN1 (downregulated)	hsa-miR-302a-3p	RP11-383H13.1
TOMM40 (downregulated)	hsa-miR-194-5p	CTB-89H12.4;KCNQ1OT1
TUBB4B (downregulated)	hsa-miR-138-5p	KCNQ1OT1;TSIX
	hsa-miR-34a-5p	AC004951.6;AC092535.3;KCNQ1OT1;LINC00662;MIR4534;PCBP2-OT1;RP11-693J15.5
	hsa-miR-494-3p	
ARFGAP3 (upregulated)	hsa-miR-494-3p	
CAPN2 (upregulated)	hsa-miR-132-3p	APTR;CASC7;CTB-89H12.4;KCNIP4-IT1;KCNQ1OT1;NEAT1;RP11-26J3.3;XIST;XLOC_006753;YEATS2-AS1
	hsa-miR-494-3p	
	hsa-miR-374a-5p	CTC-444N24.11;CTD-2561J22.5;RP11-613D13.5;TRG-AS1;XIST;XLOC_004545;XLOC_006322;ZNRD1-AS1
CP (upregulated)	hsa-miR-34a-5p	AC004951.6;AC092535.3;KCNQ1OT1;LINC00662;MIR4534;PCBP2-OT1;RP11-693J15.5
	hsa-miR-34b-5p	KCNQ1OT1;RP11-458F8.4;TSIX;XIST
	hsa-miR-34c-5p	KCNQ1OT1;LINC01000;MIR4534
	hsa-miR-449a	KCNQ1OT1;MIR4534;XIST
	hsa-miR-449b-5p	KCNQ1OT1;MIR4534;XIST
DYNLT1 (upregulated)	hsa-miR-34a-5p	AC004951.6;AC092535.3;KCNQ1OT1;LINC00662;MIR4534;PCBP2-OT1;RP11-693J15.5
	hsa-miR-449a	KCNQ1OT1;MIR4534;XIST
GFAP (upregulated)	hsa-miR-34a-5p	AC004951.6;AC092535.3;KCNQ1OT1;LINC00662;MIR4534;PCBP2-OT1;RP11-693J15.5
HSPB8 (upregulated)	hsa-miR-126-5p	AC096772.6;C14orf23;C1QTNF3-AMACR;CH17-262A2.1;DLX6-AS1;FAM201A;KCNQ1OT1;LINC01004;LINC01420;LL22NC03-2H8.5;NEAT1;RP11-177G23.2;RP11-707A18.1;RP11-946L20.2;RP4-740C4.7;TTTY15;XLOC_001417;XLOC_003971;XLOC_005753;XLOC_008295;XLOC_010463

(Continued)

TABLE 8 | Continued

AD-associate DEGs	Other neurodegenerative disease-specific miRNAs associated with genes	lncRNAs associated with miRNAs
	hsa-miR-485-5p	CTA-342B11.3;GS1-124K5.11;KCNQ1OT1;MIR4534;RP11-266K22.2;RP11-504P24.8;RP11-658F2.8;RP1-309I22.2;RP5-1014D13.2;XLOC_013174;XLOC_013274
	hsa-miR-494-3p	
	hsa-miR-374a-5p	CTC-444N24.11;CTD-2561J22.5;RP11-613D13.5;TRG-AS1;XIST;XLOC_004545;XLOC_006322;ZNRD1-AS1
IQCK (upregulated)	hsa-miR-7-5p	AC005154.6;DLX6-AS1;KCNQ1OT1;LINC01233;LINC01314;MIR4534;OIP5-AS1;OIP5-AS1;RP11-679B19.1;RP1-309I22.2;XIST
LAP3 (upregulated)	hsa-miR-494-3p	
	hsa-miR-449a	KCNQ1OT1;MIR4534;XIST
	hsa-miR-449b-5p	KCNQ1OT1;MIR4534;XIST
MAN2A1 (upregulated)	hsa-miR-7-5p	AC005154.6;DLX6-AS1;KCNQ1OT1;LINC01233;LINC01314;MIR4534;OIP5-AS1;OIP5-AS1;RP11-679B19.1;RP1-309I22.2;XIST
	hsa-miR-194-5p	CTB-89H12.4;KCNQ1OT1
MT1M (upregulated)	hsa-miR-374a-5p	CTC-444N24.11;CTD-2561J22.5;RP11-613D13.5;TRG-AS1;XIST;XLOC_004545;XLOC_006322;ZNRD1-AS1
NPL (upregulated)	hsa-miR-374a-5p	CTC-444N24.11;CTD-2561J22.5;RP11-613D13.5;TRG-AS1;XIST;XLOC_004545;XLOC_006322;ZNRD1-AS1
PLXDC2 (upregulated)	hsa-miR-7-5p	AC005154.6;DLX6-AS1;KCNQ1OT1;LINC01233;LINC01314;MIR4534;OIP5-AS1;OIP5-AS1;RP11-679B19.1;RP1-309I22.2;XIST
	hsa-miR-374a-5p	CTC-444N24.11;CTD-2561J22.5;RP11-613D13.5;TRG-AS1;XIST;XLOC_004545;XLOC_006322;ZNRD1-AS1
PRDX1 (upregulated)	hsa-miR-485-3p	HCG11;LINC00657;RP11-482H16.1;RP11-95O2.1;RP3-445N2.1;XLOC_004244
	hsa-miR-126-3p	
	hsa-miR-34a-5p	AC004951.6;AC092535.3;KCNQ1OT1;LINC00662;MIR4534;PCBP2-OT1;RP11-693J15.5
PRDX6 (upregulated)	hsa-miR-34a-5p	AC004951.6;AC092535.3;KCNQ1OT1;LINC00662;MIR4534;PCBP2-OT1;RP11-693J15.5
RAB10 (upregulated)	hsa-miR-19a-3p	CASC7;FAM201A;H19;KCNA3;KCNQ1OT1;RP11-337C18.8;RP11-523G9.3;SNHG14
	hsa-miR-19b-3p	CASC7;FAM201A;H19;KCNA3;KCNQ1OT1;LINC00094;RP11-337C18.8;SNHG14
SEPP1 (upregulated)	hsa-miR-218-5p	DYX1C1-CCPG1;INO80B-WBP1;KCNQ1OT1;RP11-166D19.1;RP11-679B19.2;RP4-621B10.8;SNHG23;XLOC_004695;XLOC_010885
	hsa-miR-194-5p	CTB-89H12.4;KCNQ1OT1
	hsa-miR-34b-5p	KCNQ1OT1;RP11-458F8.4;TSIX;XIST
SERPINA3 (upregulated)	hsa-miR-34a-5p	AC004951.6;AC092535.3;KCNQ1OT1;LINC00662;MIR4534;PCBP2-OT1;RP11-693J15.5
	hsa-miR-34c-5p	KCNQ1OT1;LINC01000;MIR4534
	hsa-miR-448	
SLC16A9 (upregulated)	hsa-miR-212-3p	CASC7;CTB-89H12.4;NEAT1;RP11-26J3.3;XIST;XLOC_006753
	hsa-miR-374a-5p	CTC-444N24.11;CTD-2561J22.5;RP11-613D13.5;TRG-AS1;XIST;XLOC_004545;XLOC_006322;ZNRD1-AS1
SRSF6 (upregulated)	hsa-miR-19a-3p	CASC7;FAM201A;H19;KCNA3;KCNQ1OT1;RP11-337C18.8;RP11-523G9.3;SNHG14
	hsa-miR-139-5p	CTC-365E16.1;CTC-444N24.11;HOXA10-HOXA9;KCNQ1OT1;NR2F1-AS1;PWAR6;RMST;RP11-215G15.5;RP13-582O9.5;XLOC_009913
	hsa-miR-494-3p	
	hsa-miR-34a-5p	AC004951.6;AC092535.3;KCNQ1OT1;LINC00662;MIR4534;PCBP2-OT1;RP11-693J15.5
TAC1 (upregulated)	hsa-miR-212-3p	CASC7;CTB-89H12.4;NEAT1;RP11-26J3.3;XIST;XLOC_006753

and was detected to be upregulated in our study. Therefore, this validates our findings in AD. It also verifies that MYC and *SERPINA3* have an activation relationship. This activation relationship is also verified in the GEO dataset GSE16759. However, in GSE97760, the result is different to ours and GSE16759, which may be due to different samples (The samples in GSE16759 were the tissues, however the samples in GSE97760 were blood).

There were 173 SNPs identified as being associated with 40 AD-associated DEGs, which were in turn regulated by AD-associated miRNAs. This enhances the relevance of these 173 SNPs in AD (**Table S13**). The function of these 173 SNPs

TABLE 9 | AD-associate miRNAs associated with other neurodegenerative disease-associate DEGs.

Other neurodegenerative disease-associate DEGs	AD-associate miRNAs	lncRNAs associated with miRNAs
MAP1A	hsa-miR-24-3p	CTA-292E10.9;CTC-273B12.8;GABPB1-AS1;LINC00662;LOC388692;MIR4534;RP11-54O7.1;XLOC_006242;XLOC_008461;XLOC_011313;
	hsa-miR-497-5p	AC005540.3;C1orf132;C1RL-AS1;FGF14-IT1;GS1-358P8.4;INO80B-WBP1;KCNQ1OT1;LINC00662;MIA-RAB4B;RP11-361F15.2;RP5-991G20.1;RP6-24A23.7;XIST;XLOC_006753;XLOC_008207;XLOC_013174;XLOC_013424
	hsa-miR-15a-5p	AC005540.3;FGF14-IT1;GS1-358P8.4;KCNQ1OT1;LINC00662;MCM3AP-AS1;RP11-361F15.2;RP11-96D1.10;RP3-508I15.20;RP5-991G20.1;RP6-24A23.7;XLOC_003546;XLOC_008207;XLOC_006753;XLOC_013174
	hsa-miR-15b-5p	AC005540.3;FGF14-IT1;GS1-358P8.4;KCNQ1OT1;LINC00662;RP11-361F15.2;RP11-96D1.10;RP3-508I15.20;RP6-24A23.7;XLOC_008207;XLOC_013174
	hsa-miR-16-5p	AC005540.3;FGF14-IT1;GS1-358P8.4;KCNQ1OT1;LINC00662;RP11-359B12.2;RP11-361F15.2;RP3-508I15.20;RP6-24A23.7;XLOC_003546;XLOC_006753;XLOC_008207;XLOC_013174
MLF2	hsa-miR-200b-3p	CTC-444N24.11;XIST;XLOC_013174
NARS	hsa-miR-15b-5p	AC005540.3;FGF14-IT1;GS1-358P8.4;KCNQ1OT1;LINC00662;RP11-361F15.2;RP11-96D1.10;RP3-508I15.20;RP6-24A23.7;XLOC_008207;XLOC_013174
ACADM	hsa-miR-128-3p	
	hsa-miR-376a-5p	KCNQ1OT1;SIK3-IT1
ACTL6A	hsa-miR-16-5p	AC005540.3;FGF14-IT1;GS1-358P8.4;KCNQ1OT1;LINC00662;RP11-359B12.2;RP11-361F15.2;RP3-508I15.20;RP6-24A23.7;XLOC_003546;XLOC_006753;XLOC_008207;XLOC_013174
	hsa-miR-18a-5p	AC000403.4;CASC7;CTB-89H12.4;IPW;KCNIP4-IT1;KCNQ1OT1;LINC00506;N4BP2L2-IT2;RP11-10E18.7;RP11-1134I14.8;RP11-147L13.14;RP11-314B1.2;RP11-361F15.2;RP11-707A18.1;RP1-309I22.2;XLOC_003971;XLOC_010463;XLOC_011185;ZNF883;ZNRD1-AS1
	hsa-miR-18b-5p	XIST;XLOC_014102
AK3	hsa-miR-16-5p	AC005540.3;FGF14-IT1;GS1-358P8.4;KCNQ1OT1;LINC00662;RP11-359B12.2;RP11-361F15.2;RP3-508I15.20;RP6-24A23.7;XLOC_003546;XLOC_006753;XLOC_008207;XLOC_013174
AMOTL2	hsa-miR-107	CASC7;KCNQ1OT1;LINC00662;MIR4534;RP11-361F15.2;RP6-24A23.7;STAG3L5P-PVRIG2P-PILRB;XLOC_006753
	hsa-miR-128-3p	
	hsa-miR-16-5p	AC005540.3;FGF14-IT1;GS1-358P8.4;KCNQ1OT1;LINC00662;RP11-359B12.2;RP11-361F15.2;RP3-508I15.20;RP6-24A23.7;XLOC_003546;XLOC_006753;XLOC_008207;XLOC_013174
ATG4C	hsa-miR-128-3p	
	hsa-miR-16-5p	AC005540.3;FGF14-IT1;GS1-358P8.4;KCNQ1OT1;LINC00662;RP11-359B12.2;RP11-361F15.2;RP3-508I15.20;RP6-24A23.7;XLOC_003546;XLOC_006753;XLOC_008207;XLOC_013174
	hsa-miR-200b-3p	CTC-444N24.11;XIST;XLOC_013174
	hsa-miR-31-5p	KCNQ1OT1;TSIX;XLOC_013174
	hsa-miR-376a-5p	KCNQ1OT1;SIK3-IT1
CAPS2	hsa-miR-33a-5p	CTC-444N24.11;KCNQ1OT1;MCF2L-AS1
FUT9	hsa-miR-33a-5p	CTC-444N24.11;KCNQ1OT1;MCF2L-AS1
HLA-DMA	hsa-miR-200b-3p	CTC-444N24.11;XIST;XLOC_013174
NUP133	hsa-miR-128-3p	
PCMTD2	hsa-miR-200b-3p	CTC-444N24.11;XIST;XLOC_013174
PLEK	hsa-miR-107	CASC7;KCNQ1OT1;LINC00662;MIR4534;RP11-361F15.2;RP6-24A23.7;STAG3L5P-PVRIG2P-PILRB;XLOC_006753
PPM1K	hsa-miR-107	CASC7;KCNQ1OT1;LINC00662;MIR4534;RP11-361F15.2;RP6-24A23.7;STAG3L5P-PVRIG2P-PILRB;XLOC_006753
	hsa-miR-128-3p	
	hsa-miR-15a-5p	AC005540.3;FGF14-IT1;GS1-358P8.4;KCNQ1OT1;LINC00662;MCM3AP-AS1;RP11-361F15.2;RP11-96D1.10;RP3-508I15.20;RP5-991G20.1;RP6-24A23.7;XLOC_003546;XLOC_008207;XLOC_006753;XLOC_013174
	hsa-miR-15b-5p	AC005540.3;FGF14-IT1;GS1-358P8.4;KCNQ1OT1;LINC00662;RP11-361F15.2;RP11-96D1.10;RP3-508I15.20;RP6-24A23.7;XLOC_008207;XLOC_013174
	hsa-miR-16-5p	AC005540.3;FGF14-IT1;GS1-358P8.4;KCNQ1OT1;LINC00662;RP11-359B12.2;RP11-361F15.2;RP3-508I15.20;RP6-24A23.7;XLOC_003546;XLOC_006753;XLOC_008207;XLOC_013174

(Continued)

TABLE 9 | Continued

Other neurodegenerative disease-associate DEGs	AD-associate miRNAs	lncRNAs associated with miRNAs
	hsa-miR-24-3p	CTA-292E10.9;CTC-273B12.8;GABPB1-AS1;LINC00662;LOC388692;MIR4534;RP11-54O7.1;XLOC_006242;XLOC_008461;XLOC_011313;
	hsa-miR-497-5p	AC005540.3;C1orf132;C1RL-AS1;FGF14-IT1;GS1-358P8.4;INO80B-WBP1;KCNQ1OT1;LINC00662;MIA-RAB4B;RP11-361F15.2;RP5-991G20.1;RP6-24A23.7;XIST;XLOC_006753;XLOC_008207;XLOC_013174;XLOC_013424
PRPF38B	hsa-miR-16-5p	AC005540.3;FGF14-IT1;GS1-358P8.4;KCNQ1OT1;LINC00662;RP11-359B12.2;RP11-361F15.2;RP3-508I15.20;RP6-24A23.7;XLOC_003546;XLOC_006753;XLOC_008207;XLOC_013174
QKI	hsa-miR-107	CASC7;KCNQ1OT1;LINC00662;MIR4534;RP11-361F15.2;RP6-24A23.7;STAG3L5P-PVRIG2P-PILRB;XLOC_006753
	hsa-miR-128-3p	
	hsa-miR-15a-5p	AC005540.3;FGF14-IT1;GS1-358P8.4;KCNQ1OT1;LINC00662;MCM3AP-AS1;RP11-361F15.2;RP11-96D1.10;RP3-508I15.20;RP5-991G20.1;RP6-24A23.7;XLOC_003546;XLOC_008207;XLOC_006753;XLOC_013174
	hsa-miR-15b-5p	AC005540.3;FGF14-IT1;GS1-358P8.4;KCNQ1OT1;LINC00662;RP11-361F15.2;RP11-96D1.10;RP3-508I15.20;RP6-24A23.7;XLOC_008207;XLOC_013174
	hsa-miR-16-5p	AC005540.3;FGF14-IT1;GS1-358P8.4;KCNQ1OT1;LINC00662;RP11-359B12.2;RP11-361F15.2;RP3-508I15.20;RP6-24A23.7;XLOC_003546;XLOC_006753;XLOC_008207;XLOC_013174
	hsa-miR-24-3p	CTA-292E10.9;CTC-273B12.8;GABPB1-AS1;LINC00662;LOC388692;MIR4534;RP11-54O7.1;XLOC_006242;XLOC_008461;XLOC_011313;
	hsa-miR-29a-3p	AC005154.6;AC006548.28;H19;KCNQ1OT1;LINC00674;MIR4697HG;NEAT1;RP11-314B1.2;RP11-582E3.6;RP4-630A11.3;THUMPD3-AS1;TTTY15;TUG1;XLOC_004366;XLOC_007942;XLOC_008295
	hsa-miR-375	KCNQ1OT1;SNHG14;SNORD116-20
	hsa-miR-497-5p	AC005540.3;C1orf132;C1RL-AS1;FGF14-IT1;GS1-358P8.4;INO80B-WBP1;KCNQ1OT1;LINC00662;MIA-RAB4B;RP11-361F15.2;RP5-991G20.1;RP6-24A23.7;XIST;XLOC_006753;XLOC_008207;XLOC_013174;XLOC_013424
RNF19A	hsa-miR-107	CASC7;KCNQ1OT1;LINC00662;MIR4534;RP11-361F15.2;RP6-24A23.7;STAG3L5P-PVRIG2P-PILRB;XLOC_006753
	hsa-miR-29a-3p	AC005154.6;AC006548.28;H19;KCNQ1OT1;LINC00674;MIR4697HG;NEAT1;RP11-314B1.2;RP11-582E3.6;RP4-630A11.3;THUMPD3-AS1;TTTY15;TUG1;XLOC_004366;XLOC_007942;XLOC_008295
SLC44A1	hsa-miR-24-3p	CTA-292E10.9;CTC-273B12.8;GABPB1-AS1;LINC00662;LOC388692;MIR4534;RP11-54O7.1;XLOC_006242;XLOC_008461;XLOC_011313
SPP1	hsa-miR-16-5p	AC005540.3;FGF14-IT1;GS1-358P8.4;KCNQ1OT1;LINC00662;RP11-359B12.2;RP11-361F15.2;RP3-508I15.20;RP6-24A23.7;XLOC_003546;XLOC_006753;XLOC_008207;XLOC_013174
STARD7	hsa-miR-31-5p	KCNQ1OT1;TSIX;XLOC_013174
	hsa-miR-433-3p	
STOM	hsa-miR-107	CASC7;KCNQ1OT1;LINC00662;MIR4534;RP11-361F15.2;RP6-24A23.7;STAG3L5P-PVRIG2P-PILRB;XLOC_006753
	hsa-miR-128-3p	
	hsa-miR-15a-5p	AC005540.3;FGF14-IT1;GS1-358P8.4;KCNQ1OT1;LINC00662;MCM3AP-AS1;RP11-361F15.2;RP11-96D1.10;RP3-508I15.20;RP5-991G20.1;RP6-24A23.7;XLOC_003546;XLOC_008207;XLOC_006753;XLOC_013174
	hsa-miR-15b-5p	AC005540.3;FGF14-IT1;GS1-358P8.4;KCNQ1OT1;LINC00662;RP11-361F15.2;RP11-96D1.10;RP3-508I15.20;RP6-24A23.7;XLOC_008207;XLOC_013174
	hsa-miR-16-5p	AC005540.3;FGF14-IT1;GS1-358P8.4;KCNQ1OT1;LINC00662;RP11-359B12.2;RP11-361F15.2;RP3-508I15.20;RP6-24A23.7;XLOC_003546;XLOC_006753;XLOC_008207;XLOC_013174
	hsa-miR-497-5p	AC005540.3;C1orf132;C1RL-AS1;FGF14-IT1;GS1-358P8.4;INO80B-WBP1;KCNQ1OT1;LINC00662;MIA-RAB4B;RP11-361F15.2;RP5-991G20.1;RP6-24A23.7;XIST;XLOC_006753;XLOC_008207;XLOC_013174;XLOC_013424
SUMF1	hsa-miR-128-3p	
	hsa-miR-16-5p	AC005540.3;FGF14-IT1;GS1-358P8.4;KCNQ1OT1;LINC00662;RP11-359B12.2;RP11-361F15.2;RP3-508I15.20;RP6-24A23.7;XLOC_003546;XLOC_006753;XLOC_008207;XLOC_013174
TRIM22	hsa-miR-107	CASC7;KCNQ1OT1;LINC00662;MIR4534;RP11-361F15.2;RP6-24A23.7;STAG3L5P-PVRIG2P-PILRB;XLOC_006753
	hsa-miR-31-5p	KCNQ1OT1;TSIX;XLOC_013174

(Continued)

TABLE 9 | Continued

Other neurodegenerative disease-associate DEGs	AD-associate miRNAs	lncRNAs associated with miRNAs
TSPAN6	hsa-miR-107	CASC7;KCNQ1OT1;LINC00662;MIR4534;RP11-361F15.2;RP6-24A23.7;STAG3L5P-PVRIG2P-PILRB;XLOC_006753
	hsa-miR-16-5p	AC005540.3;FGF14-IT1;GS1-358P8.4;KCNQ1OT1;LINC00662;RP11-359B12.2;RP11-361F15.2;RP3-508I15.20;RP6-24A23.7;XLOC_003546;XLOC_006753;XLOC_008207;XLOC_013174
VPS13C	hsa-miR-107	CASC7;KCNQ1OT1;LINC00662;MIR4534;RP11-361F15.2;RP6-24A23.7;STAG3L5P-PVRIG2P-PILRB;XLOC_006753
	hsa-miR-16-5p	AC005540.3;FGF14-IT1;GS1-358P8.4;KCNQ1OT1;LINC00662;RP11-359B12.2;RP11-361F15.2;RP3-508I15.20;RP6-24A23.7;XLOC_003546;XLOC_006753;XLOC_008207;XLOC_013174
	hsa-miR-186-5p	CTA-292E10.9;CTB-89H12.4;CTC-428G20.3;MAGI2-AS3;MIR4534;NEAT1;OIP5-AS1;RP11-61A14.2;RP1-309I22.2;XIST
	hsa-miR-29a-3p	AC005154.6;AC006548.28;H19;KCNQ1OT1;LINC00674;MIR4697HG;NEAT1;RP11-314B1.2;RP11-582E3.6;RP4-630A11.3;THUMPD3-AS1;TTTY15;TUG1;XLOC_004366;XLOC_007942;XLOC_008295

TABLE 10 | The top significant common genes in GSE16759 and our AD-associated miRNA.

ID	adj.*P*-Value	*P*-Value	logFC
hsa-miR-424	0.0889	0.0011322	−3.6568626
hsa-miR-376a	0.1033	0.0068405	−3.47133
hsa-miR-186	0.1028	0.0025921	−2.5463854
hsa-miR-148b	0.1028	0.0061566	−2.2428498
hsa-miR-101	0.0889	0.000485	−1.8992436
hsa-miR-340	0.3401	0.1038393	−1.7586512
hsa-miR-29b	0.0889	0.0014182	−1.6383336
hsa-miR-15a	0.1028	0.0040077	−1.524008
hsa-miR-137	0.1262	0.0127089	−1.4923006
hsa-miR-130a	0.1028	0.0066478	−1.4733294
hsa-miR-29c	0.1033	0.0069833	−1.4723696
hsa-miR-27a	0.1375	0.0155005	−1.011425

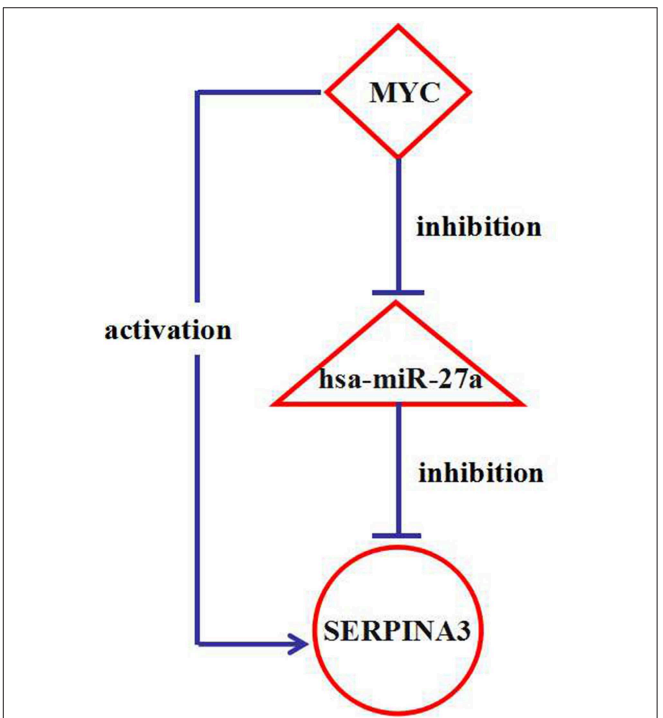

FIGURE 6 | The interaction network among a FFL nodes. The triangle-shaped node represents miRNAs, ellipse-shaped node represents genes, and diamond-shaped node represents transcription factors (TFs).

was further analyzed using the SNP annotation tool SNPnexus (http://snp-nexus.org/index.html) (Dayem Ullah et al., 2018). Several SNPs related to hsa-miR-27a were identified. Among them were SNPs rs76463641 and rs79339279, located at the *BRSK2* and *GNB5* loci, respectively, which are both already known to be AD-associated genes (Katsumata et al., 2019). Therefore, hsa-miR-27a may be an important AD epigenetic biomarker in our study.

Furthermore, our study identified several SNPs associated with five other neurodegenerative disease-associated miRNAs involved in FFL of the regulatory network. Interestingly, SNPs associated with hsa-miR-34c, hsa-miR-212, hsa-miR-34a, and hsa-miR-7 are located at known AD-associated gene loci. Thus, these four miRNAs may be associated with AD, although this requires further study for confirmation.

Although this study is strict, it has some limitations. As the power of gene analysis is affected by the sample size, especially the number of cases, the current study may not have the strongest power. In addition, not all brain regions were studied. The other limitation is that only one dataset on the HIP brain region was selected to validate the microarray results, as RNA-Seq data for the other brain regions we studied (EC and MTG) in AD is lacking. So, further study is required, possibly with larger sample sizes, more brain regions. Considering the latent effects of the identified biomolecules in the pathogenesis of AD, experimental studies should be conducted to determine the possible roles of these molecules, but are lacking. In addition, the FFL between the gene *SERPINA3*, hsa-miR-27a and the TF MYC possibly provides new candidates

TABLE 11 | The expression the gene SERPINA3, hsa-miR-27a, and TF MYC from FFL in different datasets.

Gene/miRNA symbol	GSE16759			GSE97760(mRNA)/GSE46579(miRNA)		
	adj.*P*-Value	*P*-Value	logFC	adj.*P*-Value	*P*-Value	logFC
SERPINA3	0.999	0.6698836	0.41191464	0.000878	0.0000481	2.3410491
MYC	0.988	0.2150454	0.43630728	0.541	0.323	−0.3806443
hsa-miR-27a	0.1375	0.0155005	−1.011425	0.42917903	0.576982734	−0.187196408

for treatment of AD, so further experimental verification is needed.

CONCLUSION

In this study, based on high degree and closeness centrality values in the gene expression network, eight hub genes were identified, all of which have been reported to be associated with AD. By analyzing the mTF-miRNA-gene-gTF regulatory network, 131 FFLs were identified, in which an important FFL between the gene *SERPINA3*, hsa-miR-27a, and the TF MYC was identified. Further study on the lncRNA-mediated regulatory network suggested that these lncRNAs may be significant in AD, and these have not been found in previous studies. Moreover, 173 important SNPs were identified by SNP analysis, which may be helpful for predicting AD at an earlier stage.

DATA AVAILABILITY

All the data supporting the results of this study are included in the manuscript and the related **Supplementary Documents**.

AUTHOR CONTRIBUTIONS

LS and HW designed the study. LS, SC, CZ, HW, and XS performed the data analysis. LS wrote the manuscript. HW supervised this work. All authors read and approved the final manuscript.

FUNDING

This work was supported by the Scientific Research Projects of Colleges and Universities in Hebei Province (QN2019099), the Key Project of Hebei North University (No. 120177), the Project of Hebei North University (QN2018022), and the National Innovation and Entrepreneurship Training Program for College Students (201810092001), China.

ACKNOWLEDGMENTS

We thank Catherine Perfect, MA (Cantab), from Liwen Bianji, Edanz Editing China (www.liwenbianji.cn/ac), for editing the English text of a draft of this manuscript.

SUPPLEMENTARY MATERIAL

The Supplementary Material for this article can be found online at: https://www.frontiersin.org/articles/10.3389/fnins.2019.00633/full#supplementary-material

Additional Figures | All cassette figures of the expression data after standardization.

Table S1 | Detailed descriptions of the samples including the brain regions, sex and mean age.

Table S2 | Detailed information on the RNA-Seq samples collected from GEO data GSE67333.

Table S3 | Results of sub-meta-analysis of EC brain regions on males and females.

Table S4 | Results of sub-meta-analysis of HIP brain regions on males and females.

Table S5 | Results of sub-meta-analysis of MTG brain regions on males and females.

Table S6 | Detailed information on the DEGs in RNA-Seq data set GSE67333.

Table S7 | Detailed information on the differentially expressed miRNAs from GEO data GSE16759.

Table S8 | gTFs associated with AD-associated DEGs.

Table S9 | gTFs associated with other neurodegenerative disease-associated DEGs.

Table S10 | mTFs associated with AD-associated miRNAs.

Table S11 | mTFs associated with other neurodegenerative disease-associated miRNAs.

Table S12 | Feed-forward loop from the mTF–miRNA–gene–gTF regulatory networks.

Table S13 | Important SNPs in AD and their related AD-associated miRNAs and genes.

REFERENCES

Almeida, J. F. F., Dos Santos, L. R., Trancozo, M., and de Paula, F. (2018). Updated meta-analysis of Bin1, Cr1, Ms4a6a, Clu, and Abca7 variants in Alzheimer's disease. *J. Mol. Neurosci.* 64, 471–477. doi: 10.1007/s12031-018-1045-y

Bagyinszky, E., Lee, H. M., Van Giau, V., Koh, S. B., Jeong, J. H., An, S. S. A., et al. (2018). Psen1 P.Thr116ile variant in two korean families with young onset Alzheimer's disease. *Int. J. Mol. Sci.* 19:E2604. doi: 10.3390/ijms19092604

Berchtold, N. C., Coleman, P. D., Cribbs, D. H., Rogers, J., Gillen, D. L., and Cotman, C. W. (2013). Synaptic genes are extensively downregulated across multiple brain regions in normal human aging and Alzheimer's disease. *Neurobiol. Aging* 34, 1653–1661. doi: 10.1016/j.neurobiolaging.2012.11.024

Berto, S., Usui, N., Konopka, G., and Fogel, B. L. (2016). Elavl2-regulated transcriptional and splicing networks in human neurons link neurodevelopment and autism. *Hum. Mol. Genet.* 25, 2451–2464. doi: 10.1093/hmg/ddw110

Blalock, E. M., Geddes, J. W., Chen, K. C., Porter, N. M., Markesbery, W. R., and Landfield, P. W. (2004). Incipient Alzheimer's disease: microarray correlation analyses reveal major transcriptional and tumor suppressor responses. *Proc. Natl. Acad. Sci. U.S.A.* 101, 2173–2178. doi: 10.1073/pnas.0308512100

Bruno, A. E., Li, L., Kalabus, J. L., Pan, Y., Yu, A., and Hu, Z. (2012). Mirdsnp: a database of disease-associated SNPs and microRNA target sites on 3'utrs of human genes. *BMC Genomics* 13:44. doi: 10.1186/1471-2164-13-44

Chee, L. Y., and Cumming, A. (2018). Polymorphisms in the cholinergic receptors muscarinic (Chrm2 and Chrm3) genes and Alzheimer's disease. *Avicenna J. Med. Biotechnol.* 10, 196–199.

Davis, S., and Meltzer, P. S. (2007). Geoquery: a bridge between the Gene Expression Omnibus (Geo) and bioconductor. *Bioinformatics* 23, 1846–1847. doi: 10.1093/bioinformatics/btm254

Dayem Ullah, A. Z., Oscanoa, J., Wang, J., Nagano, A., Lemoine, N. R., and Chelala, C. (2018). Snpnexus: assessing the functional relevance of genetic variation to facilitate the promise of precision medicine. *Nucleic Acids Res.* 46, W109–W113. doi: 10.1093/nar/gky399

Deane, R., Sagare, A., Hamm, K., Parisi, M., LaRue, B., Guo, H., et al. (2005). Igg-assisted age-dependent clearance of Alzheimer's amyloid beta peptide by the blood-brain barrier neonatal Fc receptor. *J. Neurosci.* 25, 11495–11503. doi: 10.1523/JNEUROSCI.3697-05.2005

Derkow, K., Rossling, R., Schipke, C., Kruger, C., Bauer, J., Fahling, M., et al. (2018). Distinct expression of the neurotoxic microRNA family Let-7 in the cerebrospinal fluid of patients with Alzheimer's disease. *PLoS ONE* 13:e0200602. doi: 10.1371/journal.pone.0200602

Durrenberger, P. F., Fernando, F. S., Kashefi, S. N., Bonnert, T. P., Seilhean, D., Nait-Oumesmar, B., et al. (2015). Common mechanisms in neurodegeneration and neuroinflammation: a BrainNet Europe gene expression microarray study. *J. Neural Transm.* 122, 1055–1068. doi: 10.1007/s00702-014-1293-0

El Kadmiri, N., Slassi, I., El Moutawakil, B., Nadifi, S., Tadevosyan, A., Hachem, A., et al. (2014). Glyceraldehyde-3-phosphate dehydrogenase (Gapdh) and Alzheimer's disease. *Pathol. Biol.* 62, 333–336. doi: 10.1016/j.patbio.2014.08.002

Ferrer, I., Blanco, R., Carmona, M., and Puig, B. (2001). Phosphorylated C-Myc expression in Alzheimer disease, Pick's disease, progressive supranuclear palsy and corticobasal degeneration. *Neuropathol. Appl. Neurobiol.* 27, 343–351. doi: 10.1046/j.1365-2990.2001.00348.x

Fogel, G. B., Weekes, D. G., Varga, G., Dow, E. R., Craven, A. M., Harlow, H. B., et al. (2005). A statistical analysis of the transfac database. *Bio Systems.* 81, 137–154. doi: 10.1016/j.biosystems.2005.03.003

Gaughwin, P. M., Ciesla, M., Lahiri, N., Tabrizi, S. J., Brundin, P., and Bjorkqvist, M. (2011). Hsa-Mir-34b Is a plasma-stable microRNA that is elevated in pre-manifest Huntington's disease. *Hum. Mol. Genet.* 20, 2225–2237. doi: 10.1093/hmg/ddr111

Guan, F., Gu, J., Hu, F., Zhu, Y., and Wang, W. (2012). Association between Alpha1-antichymotrypsin signal peptide−15a/T polymorphism and the risk of Alzheimer's disease: a meta-analysis. *Mol. Biol. Rep.* 39, 6661–6669. doi: 10.1007/s11033-012-1472-8

Guerreiro, C., Silva, B., Crespo, A. C., Marques, L., Costa, S., Timoteo, A., et al. (2015). Decrease in App and Cp mRNA expression supports impairment of iron export in Alzheimer's disease patients. *Biochim. Biophys. Acta* 1852, 2116–2122. doi: 10.1016/j.bbadis.2015.07.017

Hokama, M., Oka, S., Leon, J., Ninomiya, T., Honda, H., Sasaki, K., et al. (2014). Altered expression of diabetes-related genes in Alzheimer's disease brains: the Hisayama study. *Cereb. Cortex* 24, 2476–2488. doi: 10.1093/cercor/bht101

Huttenrauch, M., Ogorek, I., Klafki, H., Otto, M., Stadelmann, C., Weggen, S., et al. (2018). Glycoprotein Nmb: a novel Alzheimer's disease associated marker expressed in a subset of activated microglia. *Acta Neuropathol. Commun.* 6:108. doi: 10.1186/s40478-018-0612-3

Kamphuis, W., Kooijman, L., Orre, M., Stassen, O., Pekny, M., and Hol, E. M. (2015). Gfap and vimentin deficiency alters gene expression in astrocytes and microglia in wild-type mice and changes the transcriptional response of reactive glia in mouse model for Alzheimer's disease. *Glia* 63, 1036–1056. doi: 10.1002/glia.22800

Kamphuis, W., Mamber, C., Moeton, M., Kooijman, L., Sluijs, J. A., Jansen, A. H., et al. (2012). Gfap isoforms in adult mouse brain with a focus on neurogenic astrocytes and reactive astrogliosis in mouse models of Alzheimer disease. *PLoS ONE* 7:e42823. doi: 10.1371/journal.pone.0042823

Karagkouni, D., Paraskevopoulou, M. D., Chatzopoulos, S., Vlachos, I. S., Tastsoglou, S., Kanellos, I., et al. (2018). Diana-tarbase V8: a decade-long collection of experimentally supported miRNA-gene interactions. *Nucleic Acids Res.* 46, D239–D245. doi: 10.1093/nar/gkx1141

Karch, C. M., and Goate, A. M. (2015). Alzheimer's disease risk genes and mechanisms of disease pathogenesis. *Biol. Psychiatry* 77, 43–51. doi: 10.1016/j.biopsych.2014.05.006

Kardos, J., Yamamoto, K., Hasegawa, K., Naiki, H., and Goto, Y. (2004). Direct measurement of the thermodynamic parameters of amyloid formation by isothermal titration calorimetry. *J. Biol. Chem.* 279, 55308–55314. doi: 10.1074/jbc.M409677200

Katsumata, Y., Nelson, P. T., Estus, S., and Fardo, D. W. (2019). Translating Alzheimer's disease-associated polymorphisms into functional candidates: a survey of IGAP genes and SNPs. *Neurobiol. Aging* 74, 135–146. doi: 10.1016/j.neurobiolaging.2018

Kawamura, N. (2014). [Neurofascin: a novel target for combined central and peripheral demyelination]. *Rinsho Shinkeigaku* 54, 978–980. doi: 10.5692/clinicalneurol.54.978

Kelemen, L. E., Brenton, J. D., Parkinson, C., H. C. W., Piskorz, A. M., and Csizmadi I, et al. (2014). Conditions associated with circulating tumor-associated folate receptor 1 protein in healthy men and women. *PLoS ONE* 9:e96542. doi: 10.1371/journal.pone.0096542

Kumar, S., and Reddy, P. H. (2018). Microrna-455-3p as a potential biomarker for Alzheimer's disease: an update. *Front. Aging Neurosci.* 10:41. doi: 10.3389/fnagi.2018.00041

Leidinger, P., Backes, C., Deutscher, S., Schmitt, K., Mueller, S. C., Frese, K., et al. (2013). A blood based 12- miRNA signature of Alzheimer disease patients. *Genome Biol.* 14:R78. doi: 10.1186/gb-2013-14-7-r78

Li, X., Alafuzoff, I., Soininen, H., Winblad, B., and Pei, J. J. (2005). Levels of mtor and its downstream targets 4e-Bp1, Eef2, and Eef2 kinase in relationships with Tau in Alzheimer's disease brain. *FEBS J.* 272, 4211–4220. doi: 10.1111/j.1742-4658.2005.04833.x

Li, X., Zhu, X., Zhang, W., Yang, F., Hui, J., Tan, J., et al. (2018). The etiological effect of a new low-frequency Esr1 variant on mild cognitive impairment and Alzheimer's disease: a population-based study. *Aging* 10, 2316–2337. doi: 10.18632/aging.101548

Lin, J., Spidel, J. L., Maddage, C. J., Rybinski, K. A., Kennedy, R. P., Krauthauser, C. L., et al. (2013). The antitumor activity of the human Folr1-specific monoclonal antibody, farletuzumab, in an ovarian cancer mouse model is mediated by antibody-dependent cellular cytotoxicity. *Cancer Biol. Ther.* 14, 1032–1038. doi: 10.4161/cbt.26106

Liu, F. F., Zhang, Z., Chen, W., Gu, H. Y., and Yan, Q. J. (2018). Regulatory mechanism of Microrna-377 on Cdh13 expression in the cell model of Alzheimer's disease. *Eur. Rev. Med. Pharmacol. Sci.* 22, 2801–2808. doi: 10.26355/eurrev_201805_14979

Liu, J., Hoppman, N., O'Connell, J. R., Wang, H., Streeten, E. A., McLenithan, J. C., et al. (2012). A functional haplotype in Eif2ak3, an Er stress sensor, is associated with lower bone mineral density. *J. Bone Miner. Res.* 27, 331–341. doi: 10.1002/jbmr.549

Liu, Q. Y., Yu, J. T., Miao, D., Ma, X. Y., Wang, H. F., Wang, W., et al. (2013). An exploratory study on Stx6, Mobp, Mapt, and Eif2ak3 and late-onset Alzheimer's disease. *Neurobiol. Aging* 34, 1519.e13–1519.e17. doi: 10.1016/j.neurobiolaging.2012

Liu, Y., Chen, Q., Liu, X., Dou, M., Li, S., Zhou, J., et al. (2016). Genetic Association of Chat Rs3810950 and Rs2177369 polymorphisms with the risk of Alzheimer's disease: a meta-analysis. *Biomed Res. Int.* 2016:9418163. doi: 10.1155/2016/9418163

Manzine, P. R., Pelucchi, S., Horst, M. A., Vale, F. A. C., Pavarini, S. C. I., Audano, M., et al. (2018). MicroRNA 221 targets adam10 mRNA and is downregulated in Alzheimer's disease. *J. Alzheimers. Dis.* 61, 113–123. doi: 10.3233/JAD-170592

Martins-de-Souza, D., Guest, P. C., Mann, D. M., Roeber, S., Rahmoune, H., Bauder, C., et al. (2012). Proteomic analysis identifies dysfunction in cellular transport, energy, and protein metabolism in different brain regions of atypical frontotemporal lobar degeneration. *J. Proteome Res.* 11, 2533–2543. doi: 10.1021/pr2012279

Miller, J. A., Woltjer, R. L., Goodenbour, J. M., Horvath, S., and Geschwind, D. H. (2013). Genes and pathways underlying regional and cell type changes in Alzheimer's disease. *Genome Med.* 5:48. doi: 10.1186/gm452

Moradifard, S., Hoseinbeyki, M., Ganji, S. M., and Minuchehr, Z. (2018). Analysis of microRNA and gene expression profiles in Alzheimer's disease: a meta-analysis approach. *Sci. Rep.* 8:4767. doi: 10.1038/s41598-018-20959-0

Mus, E., Hof, P. R., and Tiedge, H. (2007). Dendritic Bc200 RNA in aging and in Alzheimer's disease. *Proc. Natl. Acad. Sci. U.S.A.* 104, 10679–10684. doi: 10.1073/pnas.0701532104

Nahorski, M. S., Al-Gazali, L., Hertecant, J., Owen, D. J., Borner, G. H., Chen, Y. C., et al. (2015). A novel disorder reveals clathrin heavy chain-22 is essential for human pain and touch development. *Brain* 138, 2147–2160. doi: 10.1093/brain/awv149

Ning, S., Zhao, Z., Ye, J., Wang, P., Zhi, H., Li, R., et al. (2014). Lincsnp: a database of linking disease-associated SNPs to human large intergenic non-coding RNAs. *BMC Bioinformatics* 15:152. doi: 10.1186/1471-2105-15-152

Nunez-Iglesias, J., Liu, C. C., Morgan, T. E., Finch, C. E., and Zhou, X. J. (2010). Joint genome-wide profiling of miRNA and mRNA expression in Alzheimer's disease cortex reveals altered miRNA regulation. *PLoS ONE* 5:e8898. doi: 10.1371/journal.pone.0008898

Nyarko, J. N. K., Quartey, M. O., Pennington, P. R., Heistad, R. M., Dea, D., Poirier, J., et al. (2018). Profiles of beta-amyloid peptides and key secretases in brain autopsy samples differ with sex and apoe Epsilon4 status: impact for risk and progression of Alzheimer disease. *Neuroscience* 373, 20–36. doi: 10.1016/j.neuroscience.2018.01.005

Olah, J., Vincze, O., Virok, D., Simon, D., Bozso, Z., Tokesi, N., et al. (2011). Interactions of pathological hallmark proteins: tubulin polymerization promoting Protein/P25, beta-amyloid, and alpha-synuclein. *J. Biol. Chem.* 286, 34088–34100. doi: 10.1074/jbc.M111.243907

Ong, K. L., Leung, R. Y., Wong, L. Y., Cherny, S. S., Sham, P. C., Lam, T. H., et al. (2008). Association of a polymorphism in the Lipin 1 gene with systolic blood pressure in men. *Am. J. Hypertens.* 21, 539–545. doi: 10.1038/ajh.2008.21

Paraskevopoulou, M. D., Vlachos, I. S., Karagkouni, D., Georgakilas, G., Kanellos, I., Vergoulis, T., et al. (2016). Diana-Lncbase V2: indexing microRNA targets on non-coding transcripts. *Nucleic Acids Res.* 44, D231–D238. doi: 10.1093/nar/gkv1270

Pascual-Caro, C., Berrocal, M., Lopez-Guerrero, A. M., Alvarez-Barrientos, A., Pozo-Guisado, E., Gutierrez-Merino, C., et al. (2018). Stim1 deficiency is linked to Alzheimer's disease and triggers cell death in Sh-Sy5y cells by upregulation of L-type voltage-operated Ca(2+) entry. *J. Mol. Med.* 96, 1061–1079. doi: 10.1007/s00109-018-1677-y

Perea, J. R., Lleo, A., Alcolea, D., Fortea, J., Avila, J., and Bolos, M. (2018). Decreased Cx3cl1 levels in the cerebrospinal fluid of patients with Alzheimer's disease. *Front. Neurosci.* 12:609. doi: 10.3389/fnins.2018.00609

Rankin, S. A., and Zorn, A. M. (2014). Gene regulatory networks governing lung specification. *J. Cell. Biochem.* 115, 1343–1350. doi: 10.1002/jcb.24810

Readhead, B., Haure-Mirande, J. V., Funk, C. C., Richards, M. A., Shannon, P., Haroutunian, V., et al. (2018). Multiscale analysis of independent Alzheimer's cohorts finds disruption of molecular, genetic, and clinical networks by human herpesvirus. *Neuron* 99, 64–82. doi: 10.1016/j.neuron.2018.05.023

Ren, R., Zhang, L., and Wang, M. (2018). Specific deletion Connexin43 in astrocyte ameliorates cognitive dysfunction in App/Ps1 mice. *Life Sci.* 208, 175–191. doi: 10.1016/j.lfs.2018.07.033

Shannon, P., Markiel, A., Ozier, O., Baliga, N. S., Wang, J. T., Ramage, D., et al. (2003). Cytoscape: a software environment for integrated models of biomolecular interaction networks. *Genome Res.* 13, 2498–2504. doi: 10.1101/gr.1239303

Soler-Lopez, M., Zanzoni, A., Lluis, R., Stelzl, U., and Aloy, P. (2011). Interactome mapping suggests new mechanistic details underlying Alzheimer's disease. *Genome Res.* 21, 364–376. doi: 10.1101/gr.114280.110

Stricker, R., and Reiser, G. (2014). Functions of the neuron-specific protein Adap1 (Centaurin-Alpha1) in neuronal differentiation and neurodegenerative diseases, with an overview of structural and biochemical properties of Adap1. *Biol. Chem.* 395, 1321–1340. doi: 10.1515/hsz-2014-0107

Szklarczyk, D., Gable, A. L., Lyon, D., Junge, A., Wyder, S., Huerta-Cepas, J., et al. (2019). String V11: protein-protein association networks with increased coverage, supporting functional discovery in genome-wide experimental datasets. *Nucleic Acids Res.* 47 D607–D613. doi: 10.1093/nar/gky1131

Taminau, J., Meganck, S., Lazar, C., Steenhoff, D., Coletta, A., Molter, C., et al. (2012). Unlocking the potential of publicly available microarray data using insilicodb and insilicomerging R/Bioconductor packages. *BMC Bioinformatics* 13:335.doi: 10.1186/1471-2105-13-335

Wang, D. Q., Fu, P., Yao, C., Zhu, L. S., Hou, T. Y., Chen, J. G., et al. (2018). Long non-coding RNAs, novel culprits, or bodyguards in neurodegenerative diseases. *Mol. Ther. Nucleic Acids* 10, 269–276. doi: 10.1016/j.omtn.2017.12.011

Wang, H., Li, Y., Ryder, J. W., Hole, J. T., Ebert, P. J., Airey, D. C., et al. (2018). Genome-wide RNAseq study of the molecular mechanisms underlying microglia activation in response to pathological tau perturbation in the Rtg4510 Tau transgenic animal model. *Mol. Neurodegener.* 13:65. doi: 10.1186/s13024-018-0296-y

Wang, J., Lu, M., Qiu, C., and Cui, Q. (2010). Transmir: a transcription Factor-microRNA regulation database. *Nucleic Acids Res.* 38, D119–D122. doi: 10.1093/nar/gkp803

Wang, Q., Woltjer, R. L., Cimino, P. J., Pan, C., Montine, K. S., Zhang, J., et al. (2005). Proteomic analysis of neurofibrillary tangles in Alzheimer disease identifies gapdh as a detergent-insoluble paired helical filament tau binding protein. *FASEB J.* 19, 869–871. doi: 10.1096/fj.04-3210fje

Wang, W. T., Sun, Y. M., Huang, W., He, B., Zhao, Y. N., and Chen, Y. Q. (2016). Genome-wide long non-coding RNA analysis identified circulating LncRNAs as novel non-invasive diagnostic biomarkers for gynecological disease. *Sci. Rep.* 6:23343. doi: 10.1038/srep23343

Wang, X., Kang, D. D., Shen, K., Song, C., Lu, S., Chang, L. C., et al. (2012). An R package suite for microarray meta-analysis in quality control, differentially expressed gene analysis and pathway enrichment detection. *Bioinformatics* 28, 2534–2536. doi: 10.1093/bioinformatics/bts485

Wong, T. H., van der Lee, S. J., van Rooij, J. G. J., Meeter, L. H. H., Frick, P., Melhem, S., et al. (2018). Eif2ak3 variants in dutch patients with Alzheimer's disease. *Neurobiol. Aging* 73:229. doi: 10.1016/j.neurobiolaging.2018.08.016

Yousef, G. M. (2015). Mirsnp-based approach identifies a miRNA that regulates prostate-specific antigen in an allele-specific manner. *Cancer Discov.* 5, 351–352. doi: 10.1158/2159-8290.CD-15-0230

Zhao, Y. S., Zhang, L. H., Yu, P. P., Gou, Y. J., Zhao, J., You, L. H., et al. (2018). Ceruloplasmin, a potential therapeutic agent for Alzheimer's disease. *Antioxid. Redox Signal.* 28, 1323–1337. doi: 10.1089/ars.2016.6883

Zhou, Q., Peng, D., Yuan, X., Lv, Z., Pang, S., Jiang, W., et al. (2014). Apoe and Apoc1 gene polymorphisms are associated with cognitive impairment progression in Chinese patients with late-onset Alzheimer's disease. *Neural Regen. Res.* 9, 653–660. doi: 10.4103/1673-5374.130117

Zovoilis, A., Agbemenyah, H. Y., Agis-Balboa, R. C., Stilling, R. M., Edbauer, D., Rao, P., et al. (2011). Microrna-34c is a novel target to treat dementias. *EMBO J.* 30, 4299–4308. doi: 10.1038/emboj.2011.327

Conflict of Interest Statement: CZ was employed by company Shenzhen RealOmics (Biotech) Co., Ltd.

The remaining authors declare that the research was conducted in the absence of any commercial or financial relationships that could be construed as a potential conflict of interest.